



#### EDITOR

Brendan M. Laurs (blaurs@gia.edu)

#### CONTRIBUTING EDITORS

Emmanuel Fritsch, *CNRS, Institut des Matériaux Jean Rouxel (IMN), University of Nantes, France* (fritsch@cnrs-imn.fr)

Henry A. Hänni, *SSEF, Basel, Switzerland* (gemlab@ssef.ch)

Franck Notari, *GemTechLab, Geneva, Switzerland* (franck.notari@gemtechlab.ch)

Kenneth V. G. Scarratt, *GIA Research, Bangkok, Thailand* (ken.scarratt@gia.edu)

## DIAMONDS

**Bird-like inclusion in diamond.** In March 2008, jewelry appraiser Lori Provo Coogan (Cohasset Jewelers, Cohasset, Massachusetts) was appraising a 2.41 ct diamond set in a ring when she noticed an interesting internal feature. Centered just under the table, it was comprised of a brownish orange mineral inclusion that was surrounded by tension fractures (figure 1). The distribution and shape of the fractures—which are apparently following two cleavage directions in the diamond—show a strong resemblance to a bird in flight. There are even patterns resembling feathers and a curved “beak.” The color and form of the mineral inclusion suggest that it is an eclogitic garnet (John I. Koivula, pers. comm., 2008).

Brendan M. Laurs

### A colorless diamond showing strong phosphorescence.

Unlike fluorescence to UV radiation, which is commonly observed in natural diamonds, phosphorescence is quite rare, and is mainly observed in type IIb blue diamonds, “color-change” (i.e., chameleon) diamonds, and some other colored diamonds (see J. E. Field, Ed., *The Properties of Natural and Synthetic Diamond*, Academic Press, London, 1992; S. Eaton-Magaña et al., “Fluorescence spectra of colored diamonds using a rapid, mobile spectrometer,” *Winter 2007 Gems & Gemology*, pp. 332–351). In the case of blue



Figure 1. The internal feature centered under the table facet of this diamond is composed of a mineral (probably garnet) that is surrounded by tension fractures. The overall inclusion scene (~1 mm long) shows a striking resemblance to a bird in flight. Photomicrograph by Lori Provo Coogan.

type IIb diamonds, red, orange, and blue phosphorescence with an average duration of 18 seconds has been reported (J. M. King et al., “Characterizing natural-color type IIb blue diamonds,” *Winter 1998 Gems & Gemology*, pp. 246–268). The phosphorescence behavior of these type IIb diamonds has been explained by a model of electron transition from the unknown donor to the boron acceptors, which display long decay times due to the low concentration of boron (K. Watanabe et al., “Phosphorescence in high-pressure synthetic diamond,” *Diamond and Related Materials*, Vol. 6, 1997, pp. 99–106). Phosphorescence is rarer in other diamond types, and when seen it is both less intense and of shorter duration (again, see Eaton-Magaña et al., 2007).

*Editor's note: Interested contributors should send information and illustrations to Brendan Laurs at blaurs@gia.edu or GIA, The Robert Mouawad Campus, 5345 Armada Drive, Carlsbad, CA 92008. Original photos can be returned after consideration or publication.*

GEMS & GEMOLOGY, Vol. 44, No. 2, pp. 164–190  
© 2008 Gemological Institute of America



Figure 2. This 0.54 ct colorless type IIa diamond showed strong phosphorescence. Photo by H. Ito.

Recently, a 0.54 ct colorless diamond (figure 2) was submitted to the AGT Gem Laboratory for a diamond grading and identification report. Gemological examination and Fourier-transform infrared (FTIR) spectroscopy proved that the D-color, VVS<sub>1</sub> diamond was type IIa. There was no reaction to long-wave UV radiation. However, when the diamond was examined with high-energy short-wave (<230 nm) UV radiation in the DiamondView instrument, it displayed a weak dark blue fluorescence and a very strong blue phosphorescence (figure 3). No distinct growth bands or other internal features were seen with either type of luminescence. Long-lived blue phosphorescence was also seen after exposure to a short-wave UV lamp (254 nm) in a dark room; it took about four minutes for the phosphorescence to fade entirely.

To explore possible mechanisms for the phosphorescence, photoluminescence spectra excited by both 488 and 514.5 nm lasers were recorded at liquid-nitrogen temperature. The PL spectra did not show the 776.5 nm peak that has been associated with phosphorescence in natural blue diamond (Fall 2005 Lab Notes, pp. 258–259). Instead, they

Figure 3. These DiamondView images of the 0.54 ct diamond illustrate the weak dark blue UV fluorescence (left) and strong blue phosphorescence (right).

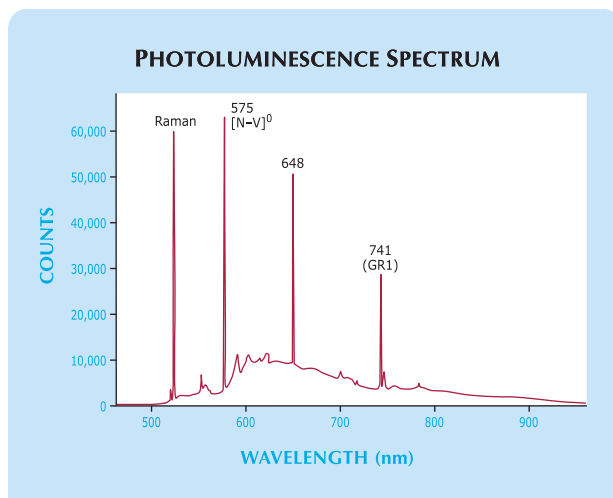
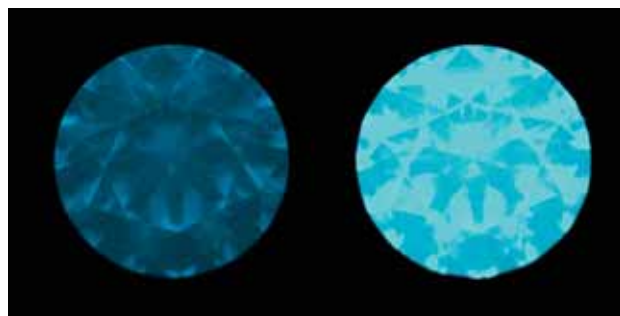


Figure 4. The photoluminescence spectrum of the type IIa diamond (here, recorded with a 488 nm laser) shows a sharp emission peak at 648 nm that may be related to its phosphorescence.

showed a strong and sharp emission peak of unknown origin at 648 nm, in addition to a GR1 peak at 741 nm and the [N-V]<sup>0</sup> center at 575 nm (figure 4).

The optical center(s) for the phosphorescence in this type IIa diamond are apparently different from those in type IIb diamonds. The detailed mechanism is unclear, but the 648 nm peak may be related to the phosphorescence in this diamond.

Taijin Lu (taijinlu@hotmail.com), Tatsuya Odaki, Kazuyoshi Yasunaga, and Hajime Uesugi  
AGT Gem Laboratory, GIA Japan, Tokyo

## COLORED STONES AND ORGANIC MATERIALS

**Almandine-spessartine from Lindi, Tanzania.** At the 2008 Tucson gem shows, Steve Ulatowski (New Era Gems, Grass Valley, California) had some attractive euhedral crystals of a new orange-red garnet from Tanzania. The crystals reportedly were mined from an area in Lindi Province, not far from the source of the pink “Imperial” pyrope-spessartine described in the Spring 2006 Gem News International (GNI) section (pp. 66–67). Mr. Ulatowski first obtained the material in January 2007, and estimates that about 1–3 kg of mixed-quality rough has been produced each month. The crystals are well-formed but typically rather small, yielding cut stones averaging <0.50 ct.

One crystal and a 1.35 ct modified round brilliant garnet (figure 5) were donated to GIA by Mr. Ulatowski, and the cut stone yielded the following properties: color—orange-red; diaphaneity—transparent; RI—1.800; SG—4.17; Chelsea filter reaction—red; and fluorescence—inert to both long- and short-wave UV radiation. The desk-model spectroscope showed weak absorption lines at 480 and 520 nm, stronger lines at 460, 505, and 565 nm, and general absorption to 440 nm. Microscopic examination



Figure 5. Lindi, Tanzania, is reportedly the source of these samples of almandine-spessartine. GIA Collection nos. 37613 (cut stone, 1.35 ct) and 37612 (crystal, 0.5 g); photo by Robert Weldon.

revealed pinpoint inclusions, short needles, and straight transparent growth lines. Energy-dispersive X-ray fluorescence (EDXRF) spectroscopy indicated major amounts of Si, Al, Mn, and Fe, and minor Mg and Ca.

The physical and chemical properties identify the garnet as almandine-spessartine, with minor pyrope and grossular components. Its refractive index and specific gravity are slightly lower than those reported for almandine-spessartine by C. M. Stockton and D. V. Manson ("A proposed new classification for gem-quality garnets," Winter 1985 *Gems & Gemology*, pp. 205–218). These differences are most likely attributable to the minor pyrope and/or grossular components.

*Elizabeth Quinn Darenius*  
([eqdarenius@aglgemlab.com](mailto:eqdarenius@aglgemlab.com))  
*American Gemological Laboratories, New York*  
*Brendan M. Laurs*

**"Red andesine" from China: Possible indication of diffusion treatment.** At the June 2007 Sainte Marie aux Mines show in France, we acquired a 1.30 ct oval-cut, orangy red stone that was sold as andesine from China (figure 6). The stone was obtained to supplement our reference gemology collection, and because it was sold for a much lower price than similar andesine-labradorite that has been represented as being from the Democratic Republic of the Congo or other localities (see, e.g., Winter 2005 GNI, pp. 356–357, and references therein).

The sample was birefringent and biaxial negative, with RIs of 1.550–1.559 and a hydrostatic SG of 2.70. These properties were consistent with plagioclase feldspar, and were closer to those of labradorite than andesine. We observed a weak orange-red/light red-orange pleochroism, and the stone was inert to both long- and short-wave UV radiation. A fairly broad absorption in the yellow region was seen with the handheld spectroscopy. Next, we measured the sample's chemical composition using a JEOL 5800 scanning electron microscope (SEM) equipped with a high-resolution Princeton Gamma Tech IMIX-PTS germanium energy-dispersive detector. The stone had the following composition (atomic percent): 19.31% Si, 11.16% Al,



Figure 6. This 1.30 ct orangy red feldspar, sold as andesine from China, proved to be labradorite with unusual color concentrations. Note the pale-colored zones in the upper portion of the stone. Photo by B. Mocquet.

4.18% Ca, 3.34% Na, 0.29% K, 0.17% Fe, and 61.5% O. These values are also consistent with a feldspar. The anorthite content of  $An_{55.5}$  [ $Ca/(Ca+Na) = 0.555$ ] corresponds to the range for labradorite ( $An_{50-70}$ ), but is close to that for andesine ( $An_{30-50}$ ).

Even with the unaided eye, it was evident that the sample had uneven coloration (again, see figure 6), particularly when viewed from the pavilion side. Microscopic examination revealed abundant parallel empty tubes or channels, as well as a few twin planes. Also seen were orangy red color concentrations around some of the channels, particularly at the terminations of those that were surface-reaching on their opposite ends (figure 7, left). It appeared as if the chromophore had diffused an equal distance in all directions from the terminations of the channels into the surrounding near-colorless areas. In addition, black pinpoint inclusions (as yet unidentified) were visible in and around the orangy red areas, but they were not present in the near-colorless zones. Hence, the stone's appearance under the microscope was very different from that of typical red andesine, which is usually almost free of inclusions and homogeneous in color. The unusual color distribution suggests a diffusion process, presumably of copper, which is a red chromophore in feldspar. Although no copper was detected in the stone, Cu in red or green feldspar is typically below the detection limit of our instrument.

With magnification, we also observed thin orange patches on the surface of some facets (figure 7, right). Because of the presence of significant red areas inside the stone, we do not believe this film contributed to the color. When these areas were analyzed with the SEM, we detected the presence of Fe in addition to the feldspar composition; the iron is probably responsible for the rust-like color of the patches. The presence of this film indicates that the stone was exposed to some type of process or treatment after faceting.

The combination of the peculiar red color distribution and the surface film residue offers evidence that the stone



Figure 7. With magnification, the labradorite shows red color concentrations around surface-reaching channels, particularly at their terminations (left; photomicrograph by B. Rondeau, magnified 40×). Some of the facets on the stone were coated with patches of a thin film containing traces of iron (right; photomicrograph by B. Mocquet, magnified ~30×).

was initially pale colored and possibly underwent diffusion treatment to acquire the orangy red color.

*Emmanuel Fritsch*

*Benjamin Rondeau*

*CNRS, Team 6112, Laboratoire de Planétologie et Géodynamique, University of Nantes, France*

*Blanca Mocquet and Yves Lulzac*

*Centre de Recherches Gemmologiques (CRG) Nantes, France*

**Orange beryl from India.** At the 2008 Tucson gem shows, Cameron McGowan and Willie Neilson (Crystalline Dream, Lake Ohau, New Zealand, and San Francisco, California) showed the *Gems & Gemology* editors some deep orange beryl. They obtained several faceted samples of this beryl (e.g., figure 8) from a local gem dealer while traveling in India in 2007. The coloration was represented as natural, and the dealer said he had collected the stones from central India over an unspecified period of time.

To investigate the origin of color in these stones, a representative 4.47 ct modified cushion step cut was loaned to American Gemological Laboratories for examination, and the following properties were determined: color—brownish orange, with weak brownish yellow and yellow-orange dichroism; diaphaneity—semitransparent to translucent; RI— $n_o = 1.587$  and  $n_e = 1.580$ ; birefringence—0.007; SG—2.72; Chelsea filter reaction—none; fluorescence—inert to long- and short-wave UV radiation; and general absorption to 450 nm and a cutoff at 670 nm visible with a desk-model spectroscope. These properties are consistent with those reported for beryl by M. O'Donoghue, Ed. (*Gems*, 6th ed., Butterworth-Heinemann, Oxford, UK, 2006, pp. 162–166).

Microscopic examination revealed numerous small needles and platelets (possibly hematite) that appeared brownish reddish orange when they occurred in larger sizes (figure 9, left), numerous two-phase (liquid and gas) inclusions, three-phase inclusions containing dark solids (figure 9, right), “fingerprints,” and fine growth tubes oriented parallel to the c-axis. Several of the two- and three-phase inclusions were surrounded by whitish film-like halos. The stone also showed evidence of clarity enhancement (fractures containing flattened gas bubbles, indicating the presence of a filler).

UV-Vis-NIR spectroscopy showed total absorption to

450 nm, a sharp peak at 455 nm, a weak shoulder at the foot of the absorption continuum at ~505 nm, and a weak broad band centered at ~835 nm. The stone's unusually deep brownish orange coloration was probably due to a combination of its orange-yellow bodycolor (most likely the result of  $O^{2-} \rightarrow Fe^{3+}$  charge transfer; see p. 94 of E. F. Fritsch and G. R. Rossman, “An update on color in gems. Part 3,” Summer 1988 *Gems & Gemology*, pp. 81–102), evidenced in the visible spectrum by the 455 nm band, and the abundant brownish reddish orange inclusions.

*Elizabeth Quinn Darenius*

Figure 8. These yellowish orange to brownish orange beryls (10.31–11.47 ct) are reportedly from central India. Photo by Robert Weldon.



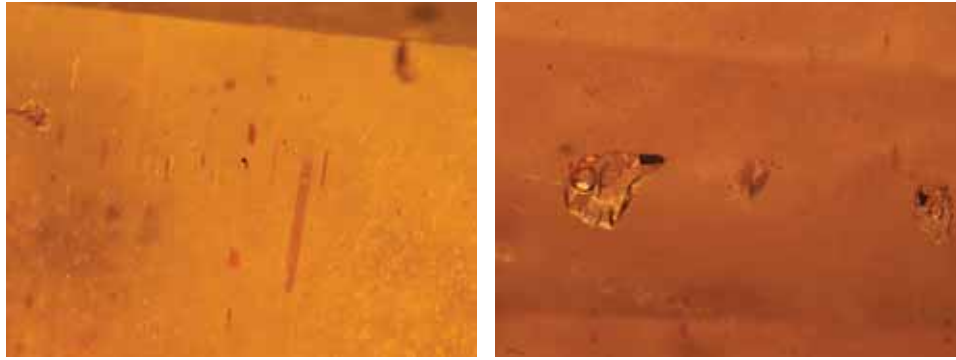


Figure 9. Brownish reddish orange needles and platelets (possibly hematite) were partially responsible for this beryl's apparent color (left). The stone contained two- and three-phase inclusions; the latter consisted of a gas bubble, a liquid, and a dark solid (right). Photomicrographs by E. Q. Darenius; magnified 65× (left) and 75× (right).

**Chromium-rich clinochlore (kämmererite) from Turkey.** Clinochlore— $(\text{Mg,Fe}^{2+})_5\text{Al}(\text{Si}_3\text{Al})\text{O}_{10}(\text{OH})_8$ —is a member of the chlorite group. Its name is derived from a combination of the Greek words *klino* (“incline”), in allusion to its monoclinic habit, and *chloros* (“green”), in reference to its most common color (J. W. Anthony et al., *Handbook of Mineralogy*, Vol. 2, Mineral Data Publishing, Tucson, AZ, 1995, p. 143). Other documented colors of clinochlore include yellow, white, and a red to purple-red Cr-rich variety that is commonly referred to as *kämmererite*. Since clinochlore has a low hardness (Mohs 2–2.5) and perfect cleavage, it is not suitable for jewelry use but is typically sold as crystal specimens or, rarely, as a collector's stone.

Alexandra Woodmansee of Rock Logic (Glencoe, Minnesota) recently loaned GIA two faceted samples (a 0.92 ct oval and a 0.52 ct cut-cornered rectangular mixed cut; figure 10) of Cr-rich clinochlore obtained from Turkey. While Cr-rich clinochlore has been reported from, among other locations, the U.S. (California, North Carolina, and Pennsylvania) and Russia (Ural Mountains), the most famous source is the Kop Mountains in eastern Turkey (see, e.g., R. Dietrich and O. Medenbach, “Kämmererite from the Kop Krom mine, Kop Dağlari, Turkey,” *Mineralogical Record*, Vol. 9, No. 5, 1978, pp. 277–287).

Examination of the two stones gave the following properties (with those for the oval cut listed first for RI and SG): color—medium-dark purplish red; RI—1.580, 1.588; hydro-

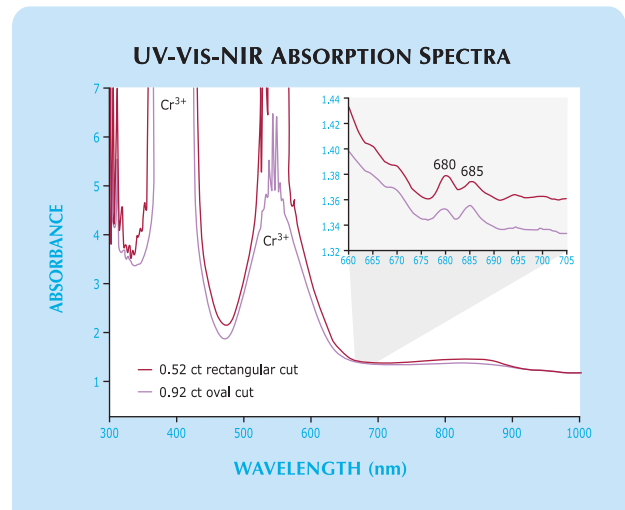
static SG—2.65, 2.67; fluorescence—inert to both long- and short-wave UV radiation; Chelsea filter reaction—positive (pink); and absorption below 440 nm and from 500–590 nm seen with a desk-model spectroscope. Microscopic examination revealed numerous fractures and cleavages, as well as crystals, needles, and clouds of tiny pinpoint inclusions. The surface of both stones showed a poor polish and many scratches and gouges, consistent with the low hardness.

The physical properties we recorded are comparable to those reported for Cr-rich clinochlore by M. O'Donoghue, Ed. (*Gems*, 6th ed., Butterworth-Heinemann, Oxford, UK, 2006, p. 420) with the exception of the SG, which O'Donoghue stated as 2.60–2.64. There are also some differences from the data presented by W. Wight (“Check-list for rare gemstones—Kämmererite,” *Canadian Gemmologist*, Vol. 17, No. 1, 1996, pp. 14–17); that article cited an absorption band at ~510–620 nm and lines at ~650 and 690 nm, as well as RIs of  $n_\alpha = 1.597$ ,  $n_\beta = 1.598$ , and  $n_\gamma = 1.599$ –1.600—but also listed other reported RI values of 1.585–1.594. Wight (1996, p. 17) further indicated that the

Figure 10. Commonly referred to as *kämmererite*, Cr-rich clinochlore is rarely seen in faceted form (here, 0.92 and 0.52 ct). Photo by Robert Weldon.



Figure 11. The UV-Vis-NIR absorption spectra for the two samples in figure 10 show absorption peaks near 400 and 550 nm, corresponding to  $\text{Cr}^{3+}$ , and two smaller peaks at ~680 and 685 nm.



low birefringence (0.003) of Cr-rich clinocllore “might result in only one line being seen in the refractometer.” This observation, coupled with the poor polish of the two stones we examined, could explain the single RI readings on our samples.

Raman analysis of these two specimens confirmed that the material was, indeed, “kämmererite.” The UV-Vis-NIR absorption spectra (figure 11) showed transmission windows in the blue and red portions of the spectrum, which are consistent with the purplish red color of the samples. The strong absorption peaks near 400 and 550 nm correlate to the features seen in the desk-model spectroscopy, and are attributed to Cr<sup>3+</sup> (R. G. Burns, *Mineralogical Applications of Crystal Field Theory*, 2nd ed., Cambridge University Press, Cambridge, UK, 1993, p. 200). Also noted were two smaller peaks at ~680 and 685 nm that may correspond to the ~690 nm line cited by Wight (1996). EDXRF analysis verified the presence of Cr as a major element in the samples, as well as Mg, Al, and Fe in major amounts, which would be expected in Cr-rich clinocllore; Ca, V, Ni, and Zn were detected in trace amounts.

According to Mrs. Woodmansee, the stones were cut from old stock. The 0.92 ct stone is one of the largest faceted specimens known to her; in general, most of the rough material is small and not suitable for cutting. Since the Turkish mine closed in 1991 due to low prices for chromium, faceted Cr-rich clinocllore will most likely continue to be extremely rare.

Karen M. Chadwick ([karen.chadwick@gia.edu](mailto:karen.chadwick@gia.edu))  
GIA Laboratory, Carlsbad

**Yellow danburite from Tanzania.** For years, gem-quality yellow danburite was known from Myanmar and Madagascar (e.g., W. Wight, “Danburite,” *Canadian Gemmologist*, Vol. 6, No. 4, 1985, pp. 110–113), and also reported from Sri Lanka (see, e.g., Spring 1986 Lab Notes, p. 47) and California (e.g., Fall 1998 Gem News, p. 220). Most recently, yellow danburite gemstones were described from a new locality in Tanzania (“Nuovi ritrovamenti: Danburite gialla di qualità gemma e gatteggiante dal Madagascar e dalla Tanzania,” *Rivista Gemmologica Italiana*, Vol. 2, No. 3, 2007, pp. 228–229).

In January 2008, we learned more about this new Tanzanian danburite from Mark Kaufman (Kaufman Enterprises, San Diego, California) and Werner Radl (Mawingu Gems, Niederwörresbach, Germany). Mr. Radl subsequently visited the deposit, which is located in the Morogoro region, in April 2008. The danburite is mined from at least two steeply dipping granitic pegmatites (e.g., figure 12) using hand tools and explosives. The pegmatites are hosted by marble, and locally contain coarse-grained pale blue-green K-feldspar (amazonite) and black tourmaline (identified as dravite-schorl by Dr. William “Skip” Simmons at the University of New Orleans by electron-microprobe analysis). The same pegmatites have reportedly produced smoky quartz and a translucent bluish violet quartz that appears to be colored by abundant micro-inclusions.

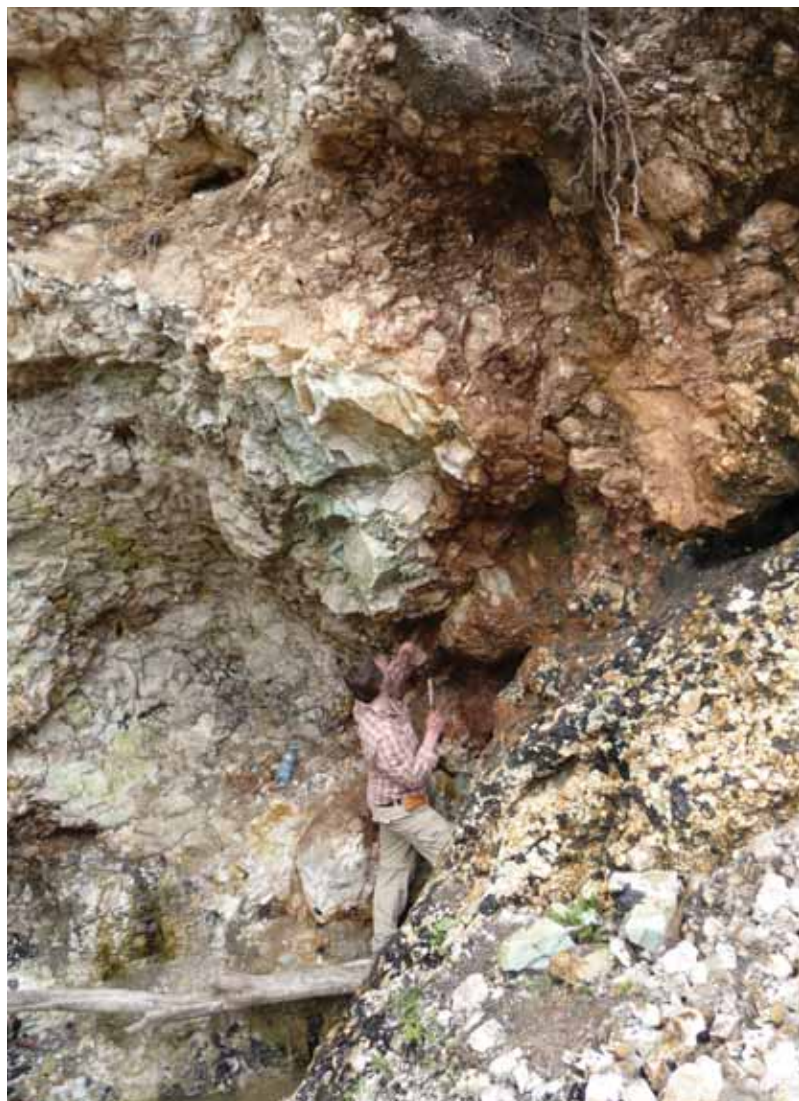


Figure 12. This granitic pegmatite in the Morogoro region of Tanzania recently produced significant quantities of yellow danburite. Courtesy of W. Radl.

Mr. Kaufman loaned GIA, for examination, two rough specimens (a 1.61 g fragment and a 12.68 g crystal) as well as two faceted (1.88 and 7.14 ct) and two cabochon-cut (8.22 and 19.41 ct) examples of the yellow danburite (e.g., figure 13). Mr. Radl showed one of us (BML) some additional faceted stones (e.g., figure 14) at the February 2008 Tucson gem shows, including a 22.48 ct oval cut, and donated a 4.37 g crystal to the Institute. Both of the crystals were tabular and twinned, resulting in a leaf-like appearance (again, see figure 13).

Examination of the cut stones gave the following properties (where they differed, values for the cabochons are noted in parentheses): color—light-to-medium yellow to orangy yellow; pleochroism—none; RI— $n_{\alpha} = 1.629\text{--}1.631$  and  $n_{\gamma} = 1.638$  (spot reading of 1.62); birefringence—0.007–0.009; hydrostatic SG—3.01 (2.97 and 3.00); inert to both long- and



Figure 13. Yellow danburite from Tanzania commonly contains abundant growth tubes, as shown by this chatoyant cabochon (8.22 ct) and twinned crystal (12.68 g). Photo by Robert Weldon.

short-wave UV radiation; and no spectrum observed with the desk-model spectroscope. Most of these properties are consistent with those given by M. O'Donoghue, Ed. (*Gems*, 6th ed., Butterworth-Heinemann, Oxford, UK, 2006, p. 403):  $n_{\alpha} = 1.627\text{--}1.633$  and  $n_{\gamma} = 1.633\text{--}1.639$ , birefringence—0.006–0.008, and SG—3.00. However, O'Donoghue reports blue to blue-green fluorescence to long-wave UV radiation, and in some stones an absorption spectrum consisting of fine lines that correspond to rare-earth elements (REEs). Wight (1985) also noted blue (and violet-blue) to blue-green fluorescence in danburite. The absence of fluorescence in the Tanzanian samples we examined—which were confirmed as danburite by Raman spectroscopy—is therefore somewhat unusual, though consistent with the Sri Lankan stones described in the Spring 1986 Lab Note.

Microscopic examination of the two faceted samples revealed long, thin, curved growth tubes (figure 15, left), as well as “fingerprints” containing angular liquid inclusions



Figure 15. Growth tubes in the Tanzanian danburite may exhibit a curved, almost hooked, appearance (left). Chatoyant material contains dense concentrations of parallel growth tubes (right). Photomicrographs by K. M. Chadwick; image width approximately 4.4 mm.



Figure 14. Transparent yellow danburite from Tanzania has been faceted into attractive gemstones (here, 9.92 and 8.67 ct). The pear shape shows distinct color zoning (yellow and near colorless). Courtesy of Mawingu Gems; photo by Robert Weldon.

and some two-phase (liquid and gas) inclusions. The presence of growth tubes and fingerprints is consistent with internal features reported in yellow danburite from Mogok, Myanmar (Summer 2007 GNI, pp. 167–168). While the two cabochons contained similar inclusions, plus a few fractures, a much denser concentration of parallel growth tubes in some stones (figure 15, right) resulted in chatoyancy (again, see figure 13).

The cause of color in yellow danburite is as yet undetermined. EDXRF analysis of five samples detected the presence of Si and Ca in major amounts, minor Sr, and traces of Fe and REEs (Ce and possibly La or Pr). Laser ablation–inductively coupled plasma–mass spectrometry (LA-ICP-MS)—performed on the two cabochons and the larger twinned crystal by GIA Laboratory research scientist Dr. Andy H. Shen—verified the presence of Sr (~450 ppm), Fe (~30 ppm), and the light rare-earth elements La (~350 ppm), Ce (~500 ppm), Pr (~30 ppm), and Nd (~60 ppm). Heavier REEs (Sm through Lu) were present in very low concentrations (<5 ppm) or were below the detection limit of the instrument. A UV-Vis-NIR spectrum collected from the larger faceted stone showed (in addition to a transmission window encompassing the yellow region) a minor absorption feature extending from ~564 to 589 nm. This feature peaked at 585 nm, which correlates with an absorption line attributed to REEs in yellow danburites from Sri Lanka (again, see the Spring 1986 Lab Note).

According to Mr. Radl, the Tanzanian danburite was first discovered in late 2006, but only small amounts were produced until late 2007. As of the February 2008 Tucson shows, he had obtained approximately 1 tonne of mixed-grade material, but less than 5 kg was of gem quality. From this small amount he had faceted ~200 carats, in clean stones weighing up to 27.8 ct (but typically <10 ct). In late February 2008, gem dealer Syed Iftikhar Hussain (Syed Trading Co., Peshawar, Pakistan) reported seeing a parcel of rough Tanzanian danburite in Bangkok consisting of 2.4 kg of chatoyant material and 1.6 kg of faceted rough, as well as an attractive cat's-eye stone weighing about 52 ct. He estimated that larger cabochons could be cut.

Karen M. Chadwick and  
Brendan M. Laurs

**Lawsonite from Marin County, California.** The mineral lawsonite [ $\text{CaAl}_2\text{Si}_2\text{O}_7(\text{OH})_2 \cdot (\text{H}_2\text{O})$ ] was first discovered in 1895, on the Tiburon Peninsula in Marin County, California. It was named in honor of Professor Andrew C. Lawson of the University of California at Berkeley (L. F. Ransome, "On lawsonite, a new rock-forming mineral from the Tiburon Peninsula," *Bulletin of the Department of Geology*, University of California Publications, Vol. 1, No. 10, 1895, pp. 301–312). Lawsonite is found in low-temperature, high-pressure metamorphic rocks formed in subduction zones, and is typically opaque, brittle, and highly included. Therefore it was a gemological treat when Steve Perry of Steve Perry Gems (Davis, California) showed us numerous samples of translucent-to-semi-transparent lawsonite at the 2008 Tucson gem shows. He obtained the material from an old mineral collection that he had recently purchased, consisting of about 320 kg of lawsonite specimens collected by a road construction mechanic on the Tiburon Peninsula. Although the time in which the specimens were collected is unknown, newspapers used for wrapping them were dated 1953.

According to Mr. Perry, the specimens consist of a matrix of glaucophane schist with small cavities containing crystals of lawsonite, pyrite, and rutile needles. Also present in the matrix of some pieces were brown garnet, chlorite, and opaque sphene. From a selection of broken lawsonite crystals, Mr. Perry arranged to cut 11 carats of faceted stones and 110 carats of cabochons. Of these, approximately 80% were "peachy" pink, 15% were grayish blue, and 5% were near colorless; less than 5% of the cabochons showed chatoyancy. Overall, less than 0.1% of the rough material was facet grade, and the vast majority ranged from translucent to opaque. The largest transparent faceted stone weighed 0.40 ct.

Mr. Perry loaned several rough and cut samples to GIA for examination, including five faceted stones and a cabochon showing chatoyancy (0.09–0.43 ct; figures 16 and 17). The following gemological properties were recorded on the faceted lawsonites: color—light pink, or near colorless to grayish blue; pleochroism—strong, in light pink and near colorless, or blue and near colorless; RI—1.664–1.687; bire-



Figure 16. These faceted lawsonites (0.09–0.18 ct) from Marin County, California, were selected to show the range of color of the faceted material. Photo by Kevin Schumacher.

fringence—0.023; SG—3.08–3.30; and fluorescence—inert to both long- and short-wave UV radiation. These properties are comparable to those reported for lawsonite by R. Webster (*Gems*, 5th ed., revised by P. G. Read, Butterworth-Heinemann, Oxford, UK, 1994, p. 349). Microscopic examination revealed numerous crystals, clouds, feathers, and "fingerprints" in all the samples. Perfect incipient cleavage planes were also present. A few samples showed areas of chips and cavities, a result of the material's brittleness. UV-Vis absorption spectroscopy revealed only a broad band centered at 450 nm. Further spectroscopic and chemical analysis would be needed to understand the cause of the various colors shown by these gems.

This is the first time cut and polished lawsonite has been seen in the GIA Laboratory.

Kevin G. Nagle ([kevin.nagle@gia.edu](mailto:kevin.nagle@gia.edu))  
GIA Laboratory, Carlsbad  
Brendan M. Laurs

Figure 17. This 0.43 ct lawsonite cabochon shows chatoyancy. Photo by Robert Weldon.





Figure 18. These Cr/V-bearing mica samples (3.33 g and 16.54 ct) from northern Pakistan were identified as consisting predominantly of paragonite. Photo by Robert Weldon.

**Green mica (paragonite) from Pakistan.** The term *green mica* usually calls to mind phlogopite or Cr-bearing muscovite (“fuchsite”), or possibly celadonite or margarite. However, Makhmout Douman (Arzawa Mineralogical Inc., New York) recently loaned GIA two samples of green mica from Pakistan—one polished stone and one piece of rough weighing 16.54 ct and 3.33 g, respectively (figure 18)—that proved to be none of these. Mr. Douman reported that the material is hosted by mica schist in a remote area about 160 km northeast of the town of Mingora (famous for producing emeralds).

Examination of the cabochon gave the following properties: color—medium bluish green; pleochroism—none; RI—1.59 (flat facet reading from base and spot reading from top); hydrostatic SG—2.89; fluorescence—faint green to long-wave and inert to short-wave UV radiation; Chelsea filter reaction—positive (pink); and a band at ~600 nm and cutoff at ~410 nm observed with a desk-model spectroscope. The physical properties (RI and SG) were consistent with those given for phlogopite and Cr-bearing muscovite, but not for celadonite or margarite, by M. E. Fleet (*Rock-Forming Minerals—Sheet Silicates: Micas*, Vol. 3A, 2nd ed., Geological Society, London, UK, 2003). The properties were also consistent with those cited by Fleet for paragonite— $\text{NaAl}_2[\text{AlSi}_3\text{O}_{10}](\text{OH})_2$ . That material is generally colorless to light yellow, but purplish red paragonite has also

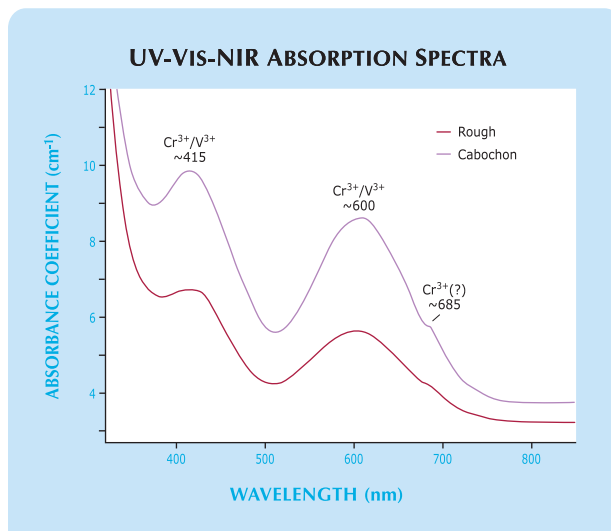


Figure 19. The unoriented UV-Vis-NIR absorption spectra of the paragonite show strong absorption peaks at ~415 and ~600 nm, corresponding to  $\text{Cr}^{3+}$  and/or  $\text{V}^{3+}$ , and a small peak at ~685 nm, probably attributable to  $\text{Cr}^{3+}$ .

been reported (e.g., Fall 1993 Gem News, p. 212). Microscopic examination of the two samples revealed a granular texture, while the piece of rough was intergrown with some off-white material (again, see figure 18).

Raman spectra collected from both the cabochon and the rough specimen gave excellent matches for the paragonite spectrum in the RRUFF database (<http://rruff.info>; sample no. R050447), and were also consistent with a spectrum for paragonite published by A. Tlili et al. (“A Raman microprobe study of natural micas,” *Mineralogical Magazine*, Vol. 53, 1989, pp. 165–179). The spectra were not consistent with phlogopite, muscovite, margarite, or celadonite. Raman spectroscopy also identified the off-white material on the rough sample as sodic plagioclase.

EDXRF analysis of both samples revealed major amounts of Na, Al, Si, and K; minor amounts of Ca, Fe, and Sr; and minor or trace amounts of Ti, V, Cr, Ga, Rb, Ba, and Pb. LA-ICP-MS analysis of the rough confirmed the presence of each of those elements, and also detected Li (not detectable by EDXRF), Mg (present in quantities too low to



Figure 20. This attractive 14.04 ct opal (left) displayed interesting and unusual lizard skin-like growth features, but it proved to be of natural origin. It exhibited bright green fluorescence to UV radiation (right). Photos by G. Choudhary.

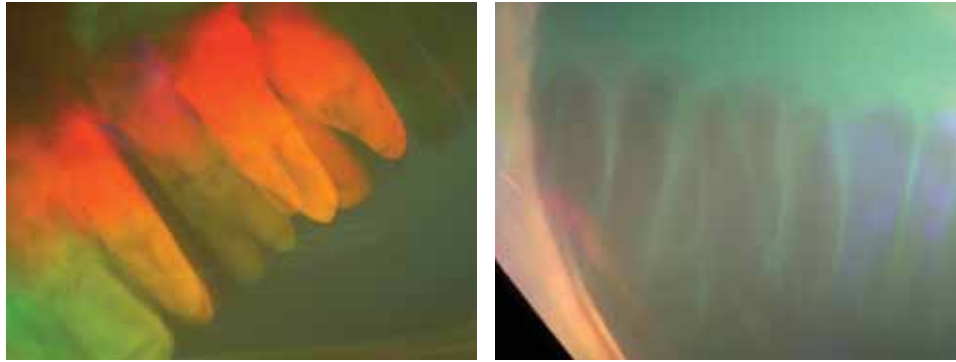


Figure 21. Distinct columnar flashes of color were seen when the opal was illuminated with a fiber-optic light (left). The columns took on a grayish appearance when the light source was placed in certain orientations (right). Note the transparent areas between the grayish zones. Photomicrographs by G. Choudhary; magnified 70× (left), 50× (right).

detect with our EDXRF instrument), and traces of several additional elements. While the elemental concentrations of the samples indicated that paragonite could be the major component, it is possible that micro-inclusions of feldspar might contribute to the excess K and Al that we detected. X-ray diffraction (XRD) analysis of the rough sample was performed by Dr. Anthony Kampf at the Natural History Museum of Los Angeles County. His results were also consistent with paragonite. We concluded on the basis of the structural and compositional evidence that the samples were indeed predominantly paragonite.

The visible region of unoriented UV-Vis-NIR spectra (figure 19) of both samples showed a transmission window at about 505–510 nm, consistent with their blue-green to bluish green color. The spectra also exhibited two areas of strong absorption at approximately 415 and 600 nm, which correspond to Cr<sup>3+</sup> and/or V<sup>3+</sup> in muscovite (see, e.g., R. G. Burns, *Mineralogical Applications of Crystal Field Theory*, 2nd ed., Cambridge University Press, Cambridge, UK, 1993). Concentrations of V and Cr obtained from our LA-ICP-MS analysis were ~280 and 580 ppm, respectively. A small peak at ~685 nm was also recorded in the absorption spectra; a similar feature at about 676 nm in Cr-bearing muscovite was attributed to Cr<sup>3+</sup> by G. H. Faye (“The optical absorption spectra of certain transition metal ions in muscovite, lepidolite, and fuchsite,” *Canadian Journal of Earth Sciences*, Vol. 5, No. 1, 1968, pp. 31–38).

According to Mr. Douman, this green mica is from an isolated discovery, from which approximately 20–30 kg/month of mixed-quality rough have been produced sea-

sonally; production is limited by the harsh conditions and remoteness of the area. Gem-quality pieces typically range from 3 to 20 g.

Karen M. Chadwick and Andy H. Shen  
GIA Laboratory, Carlsbad

**An interesting opal.** Recently, staff members at the Gem Testing Laboratory, Jaipur, India, examined an opal that exhibited an interesting and unusual growth pattern. The 14.04 ct oval cabochon (figure 20, left) had a semitransparent, colorless to milky white appearance with distinct play-of-color.

A spot RI of 1.46 and a hydrostatic SG of 2.03 were consistent with opal—natural as well as synthetic. The specimen fluoresced a striking bright green to UV radiation (figure 20, right), with a stronger reaction to short-wave than to long-wave UV.

With magnification and a fiber-optic light, the play-of-color patches appeared to be restricted to zones or planes (figure 21, left), which gave the impression of columns rising from a common base. When the light source was moved, the colors of these zones changed dramatically; in some orientations they appeared grayish (figure 21, right) and revealed the growth structure of this opal. With careful examination, some milky zones were evident between the boundaries of the columns. Viewing along the column direction, we observed a cellular growth pattern (figure 22, left). When the stone was examined while immersed in water, the cellular growth structure showed unexpected whitish zones in a net-like pattern with pseudo-hexagonal

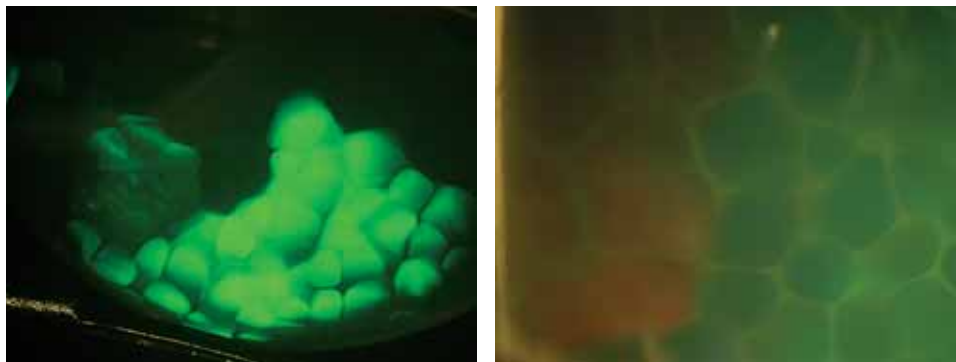


Figure 22. When the opal was viewed down the length of its columnar structure, a cellular pattern became evident in reflected light (left), and a lizard skin-like structure with pseudo-hexagonal whitish boundaries was visible when using transmitted light (right). Photomicrographs by G. Choudhary; magnified 50× (left), 80× (right).



Figure 23. A special engraving technique was used to fashion this single-strand Islamic rosary of black cultured pearls. The round ones range from 11 to 14 mm in diameter. Photo by S. Singhamroong, © Dubai Gemstone Laboratory.

boundaries (figure 22, right), which is very similar to the “lizard skin” effect observed in synthetic or imitation opals.

E. J. Gübelin and J. I. Koivula (*Photoatlas of Inclusions in Gemstones*, Vol. 2, Opinio Publishers, Basel, Switzerland, 2005, pp. 500–501) illustrated similar columnar and cellular patterns in natural opal from Nevada. However, no reports of a cellular structure with whitish boundaries were found during a literature search.

The overall features of this opal indicated natural origin, but FTIR spectroscopy was performed for confirma-



Figure 24. When examined closely, the engraved cultured pearls showed a glassy appearance. Photo by S. Singhamroong, © Dubai Gemstone Laboratory.

tion. The spectrum was similar to those reported for natural material, with an absorption band in the 5350–5000  $\text{cm}^{-1}$  region, a hump ranging from 4600 to 4300  $\text{cm}^{-1}$ , and strong absorption from approximately 4000 to 400  $\text{cm}^{-1}$ . EDXRF analysis revealed Si and traces of Ca and Fe.

This is another illustration of the importance of careful observation. Misinterpreting the lizard skin-like growth features in this opal could have resulted in a misidentification as synthetic.

Gagan Choudhary (gtl@gjepcindia.com)  
Gem Testing Laboratory, Jaipur, India

**Engraved black cultured pearls.** Several fashioning and manufacturing techniques for cultured pearls have been developed in the past decade. These include Komatsu faceted “Flower Pearls” (Summer 1997 Gem News, pp. 146–147) and “Magic Pearls” with gem inlays (Spring 2002 GNI, pp. 97–98). Recently, the Dubai Gemstone Laboratory had the opportunity to see an interesting engraving technique applied to black cultured pearls.

Umit Koruturk of Australian Pure Pearl (Sydney) submitted an attractive single strand of engraved black cultured pearls (figure 23) to the Dubai Gemstone Laboratory



Figure 25. With reflected light, it was obvious that the cultured pearls had been coated with a transparent, colorless substance (left, magnified 20 $\times$ ). Small fissures and exposure of the white shell bead nucleus were seen in areas with thin nacre (right, magnified 12 $\times$ ). Photomicrographs by S. Singhamroong, © Dubai Gemstone Laboratory.

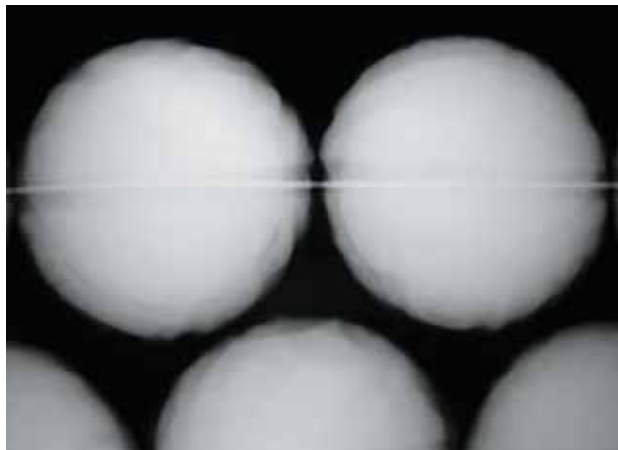


Figure 26. X-radiography revealed nacre thicknesses of only 0.3–0.6 mm in some of the engraved cultured pearls. Image by S. Singbamroong, © Dubai Gemstone Laboratory.

for an identification report. A traditional Islamic rosary, the strand consisted of 33 engraved round pearls (11–14 mm in diameter), two button-shaped pearls used as separators, and an engraved drop-shaped pearl for joining the strand. The cultured pearls had gray, brown, and black bodycolors with overtones varying from rosé to green.

On closer visual examination, the cultured pearls showed a glassy appearance (figure 24). When examined with magnification and reflected light, it was evident that they had been coated with a transparent, colorless substance (figure 25, left), possibly to improve the durability and apparent luster. Some of those with thin nacre showed small fissures and areas in the engraved patterns where the white bead nucleus was exposed (figure 25, right).

The cultured pearls were inert to long- and short-wave UV radiation. X-radiography revealed that the nacre varied from 0.3 to 1.3 mm thick, with a few having nacre in the 0.3–0.6 mm range (figure 26). UV-Vis reflectance spectra consistently revealed absorption maxima at 700 nm,

Figure 27. The five white beadless cultured pearls shown here (up to 19 mm long) were likely mantle grown in a *P. maxima* oyster. A pink Chinese freshwater cultured pearl is shown for comparison. Photo by H. A. Hänni, © SSEF.



which is characteristic of natural-color black cultured pearls from the *Pinctada margaritifera* oyster. EDXRF analysis also confirmed the absence of manganese and metals such as silver, proving the pearls were of saltwater origin and natural color.

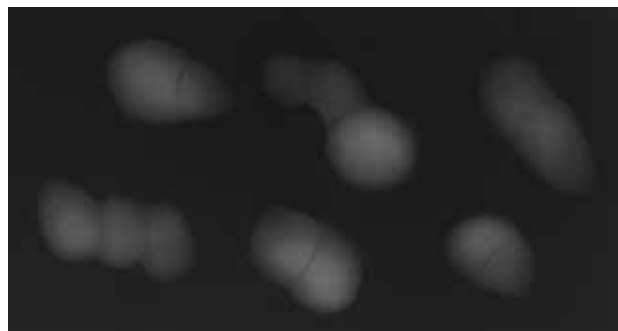
According to Umit Koruturk, the design was drawn on the cultured pearls' surface before the hand-engraving work, which utilized special tools and a unique method that requires an experienced fashioner. The fashioner can engrave from 3 to 10 pearls per day. The company has reserved about 9,000 cultured pearls for this engraving process, mainly consisting of South Sea (Indonesian) material in nearly the entire range of bodycolors and overtones. As of mid-June 2008, approximately 2,000 cultured pearls had been engraved by this technique.

Sutas Singbamroong (sssutas@dm.gov.ae)  
and Ayesha Rashid Ahmed  
Dubai Gemstone Laboratory  
Dubai, United Arab Emirates

***Pinctada maxima* cultured pearls grown beadless in the mantle.** Several lots of oddly shaped silvery white pearls (see, e.g., figure 27) arrived at the SSEF laboratory in March 2008. They were rather flat on one side, with the largest being 19 mm long. Many appeared to be intergrown, and the multiple structures were clearly visible with X-radiography (figure 28). The appearance and growth structure were strongly reminiscent of some beadless freshwater cultured pearls from China. Natural saltwater pearls only very rarely contain two centers and commonly display a more complex growth pattern.

When considering the various methods for culturing pearls, we can postulate a few options for these samples. Both freshwater (e.g., *Hyriopsis*, *Anadonta*, *Cristaria*) and saltwater (e.g., *P. maxima*, *P. margaritifera*) mollusks can be used as hosts for pearl culturing. Growth can be stimulated with a piece of mantle tissue grafted into either the gonad or the mantle. In addition, the tissue piece can be implanted with or without a bead. Thus far, a number of

Figure 28. X-radiography of the cultured pearls in figure 27 shows their composite nature with multiple centers. The dark lines mark the intergrowths. Image by H. A. Hänni, © SSEF.



combinations have been seen: Freshwater mussel + mantle grown + beadless = a Japanese Biwa cultured pearl or the classic Chinese freshwater cultured pearl. Saltwater oyster + gonad grown + bead = a product such as Akoya or South Sea cultured pearls. Less well known are South Sea “keshi” cultured pearls (saltwater oyster + gonad grown + beadless; see H. A. Hänni, “A short review of the use of ‘keshi’ as a term to describe pearls,” *Journal of Gemmology*, Vol. 30, 2006, pp. 51–58). A more recent development consists of freshwater mussels with coin-shaped beads (freshwater mussel + mantle grown + bead; see D. Fiske and J. Shepherd, “Continuity and change in Chinese freshwater pearl culture,” Summer 2007 *Gems & Gemology*, pp. 138–145).

The cultured pearls we examined appeared to be a new variation: saltwater oyster + mantle grown + beadless. These samples (again, see figure 27) showed all the characteristics of a product that was the result of tissue grafted into the mantle of *P. maxima*. It is possible that the host oysters were used for culturing two types of pearl at the same time: beaded, gonad-grown cultured pearls and these beadless mantle-grown products. That the baroque-shaped cultured pearls contained multiple centers joined into a single body reminded us of similar-appearing Chinese freshwater cultured pearls reported in the GNI entry that follows in this issue. As with the “twin” cultured pearl described in that entry, the samples documented here may have resulted from the mantle pieces being placed too close to one another, or the cultured pearls were left in their host mollusks for too long a period of time.

The trade has typically referred to beadless cultured pearls from *P. maxima* and *P. margaritifera* as “keshi.” We expect that these new products will appear under this name on the market. While South Sea and Tahitian keshis so far have consisted of gonad-grown cultured pearls formed after bead rejection, the pearls described here are obviously mantle grown, as indicated by their flattened base which suggests formation close to the shell.

Henry A. Hänni

**Twinned cultured pearl.** The SSEF laboratory is seeing an increasing number of natural pearls for examination. The majority show the typical features of saltwater natural pearls: diagnostic X-ray structures and the absence of Mn as a trace element. The identification of freshwater natural pearls is more challenging because they typically lack beads, so their shape and growth structures are usually the only characteristics that offer clues for identification. LA-ICP-MS is still not a routine technique, and research and chemical sampling are in progress.

In February 2008, we received an unusual 5.61 ct “twinned” pearl (i.e., two intergrown pearls) for identification. Unlike most such pearls, though, the two parts of the intergrowth were different colors (figure 29). There was also a broken surface on one side that suggested that a third pearl was once attached to the other two. X-radiography in two perpendicular directions (figure 30) showed



Figure 29. This bicolored freshwater cultured pearl (15 × 8 × 6 mm) is actually an intergrowth of two pearls that were undoubtedly stimulated by tissue pieces taken from different areas of the mantle of the donor mollusk. They are shown on the shell of *Hyriopsis cumingii*, the most common source of mantle tissue for freshwater pearls cultured in China. The surface of the shell illustrates the variety of nacre colors that can be produced by the mantle tissue. Photo by H. A. Hänni, © SSEF.

clear evidence that this was a beadless cultured pearl, with two typically shaped central cavities. Analysis of the Mn

Figure 30. X-radiographs of the twinned pearl show features typical of beadless cultured pearls, especially the characteristic complex-shaped central cavity. Image by H. A. Hänni, © SSEF.

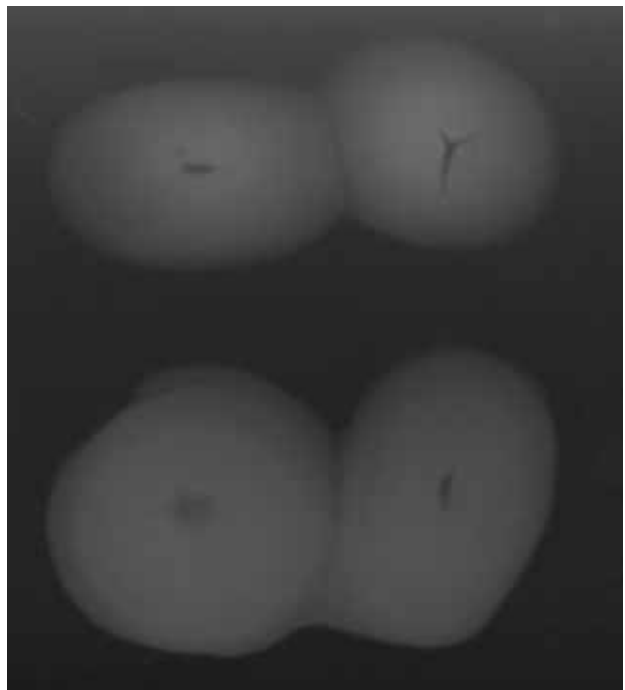




Figure 31. These pallasitic peridot specimens came from an undisclosed location in the United States. The slab measures 45 × 30 mm, and the other samples weigh 1.06, 0.50, 0.67, and 3.47 ct (from left to right; photo by Robert Weldon). The 0.36 ct cabochon in the inset shows good chatoyancy (photo by R. Stinson).

content (by luminescence to X-rays and EDXRF spectroscopy) gave results consistent with freshwater origin. We concluded that this was a beadless cultured pearl such as those produced in China.

Chinese pearl farmers typically culture freshwater pearls by grafting numerous pieces of mantle tissue in multiple closely spaced rows in the mantle of the host mollusk. The color of the resulting cultured pearl is directly related to the original location of the tissue in the donor mollusk. The bicolored nature of this sample probably resulted when tissue pieces taken from different locations of the donor mollusk were placed adjacent to one another. The “twin” resulted either because they were too close, or the cultured pearls were left in the mollusk for too long a period of time.

Henry A. Hänni

**Interplanetary cat’s-eye peridot.** Pallasite, a type of stony-iron meteorite first described in the 18th century, is known for the yellowish green olivine that can be extracted from it. Yet pallasitic peridot, the gem variety of olivine, is extremely rare. (For historical background and a gemological examination of nine faceted samples, see J. Sinkankas et al., “Peridot as an interplanetary gemstone,” Spring 1992 *Gems & Gemology*, pp. 43–51.)

At the 2008 Tucson gem shows, meteorite hunter Steve Arnold of Kingston, Arkansas, showed the *G&G* editors five pallasitic specimens: one faceted peridot, one oval peridot cabochon showing chatoyancy, a rough piece of peridot, an irregularly shaped cabochon, and a slab of pallasite con-

taining gem-quality peridot (figure 31). Using a metal detector, Mr. Arnold discovered several kilograms of the material in 2006 near a known meteorite location in the United States. He took the rough to Rick Stinson (Stinson Gemcutting Inc., Wichita, Kansas), who observed that some of the peridot was chatoyant (figure 31, inset), a phenomenon that is very rare in terrestrial peridot. According to Mr. Arnold, the American Museum of Natural History in New York later identified the cause of chatoyancy as parallel, tube-like hollow inclusions.

Peridot is a relatively soft gem material (6.5 on the Mohs scale), and the pallasitic material seems more fragile than peridot mined on Earth, perhaps due to the stress of its passage through the atmosphere and subsequent impact. In fact, a small piece of the peridot cabochon chipped off as the stone was being prepared for photography in Tucson.

Because extracting the gem-quality peridot is so difficult and destructive, Mr. Arnold estimates that less than 1% of the total weight of the recovered meteorite material will be converted into finished gemstones. So far 40 stones have been faceted, ranging from 0.20 to 1.04 ct, and only a few cabochons showing chatoyancy have been cut.

Stuart Overlin (soverlin@gia.edu)  
GIA, Carlsbad

**New rubies from central Tanzania.** At last April’s BaselWorld jewelry fair in Switzerland, the SSEF Swiss Gemmological Institute received a number of attractive rubies (e.g., figure 32) with uncommon features. The stones, which were submitted by different dealers, all had a rather saturated red hue, and their internal features indicated they were clearly unheated. The largest weighed 10.75 ct (figure 33). EDXRF qualitative chemical analysis of all the samples established that Cr and Fe were the main trace elements, while Ga was low and Ti and V were below detection limits. The client was sure of the stone’s Tanzanian origin and expected to see the country identified on the test report. Because SSEF had not seen faceted rubies with such characteristics before, it was not possible to specify the origin at that time.

However, we recalled a small parcel of rough corundum

Figure 32. These unheated rubies (2.2–3.6 ct) are apparently from a new locality in Tanzania called Winza, near the town of Mpwapwa. Photo by H. A. Hänni, © SSEF.





Figure 33. This 10.75 ct ruby from Winza has no fissures and shows no indications of heating. Courtesy of Gemburi Co., Chanthaburi, Thailand; photo by H. A. Hänni, © SSEF.

(figure 34) from a new deposit in Tanzania that was supplied in January 2008 by Werner Spaltenstein, a buyer in East Africa. These samples were represented to him as coming from the village of Winza, which is located near Mpwapwa, about 85 km east-southeast of Dodoma. The crystals and fragments displayed various habits and crystal faces, the most surprising of which was an octahedron-like variation of a rhombohedral shape (compare with H. A. Hänni and K. Schmetzer, “New rubies from the Morogoro area, Tanzania,” Fall 1991 *Gems & Gemology*, pp. 156–167). As with the crystals described by Hänni and Schmetzer (1991), the triangular faces of the Winza samples had fine lines visible with magnification that represented the surface expression of thin twin lamellae.

A comparison of the material from Winza with the cut stones examined during the Basel fair showed a similar chemical composition, and some of the inclusions were

identical. These included bent fibers that were actually hollow channels filled with a polycrystalline substance (probably secondary minerals; figure 35, left), as well as partially healed fissures consisting of idiomorphic cavities with a polycrystalline filling of white and black grains (figure 35, right). Therefore, we concluded that the rubies seen at the fair were indeed from Winza.

The faceted gems we have seen thus far from this new deposit suggest that there is considerable potential for high-quality rubies that in some cases do not need enhancement. But as with all deposits, a considerable amount of lower-quality material is also probably present—in this case, as fractured stones with blue color zones. Such corundum will likely be subject to flux-assisted heat treatment to remove the blue spots and “heal” the fractures.

Henry A. Hänni

**Ruby and sapphire mining at Winza, Tanzania.** As reported in the previous GNI entry, some fine rubies were recently produced from a new deposit at Winza in central Tanzania. In April–May 2008, these contributors undertook separate field research expeditions to the mining area to document its location, mining, and geology, and also to obtain research samples for characterization. Since foreigners are prohibited from visiting the deposit, we had to obtain permission from several government officials, who also supplied police escorts. We are grateful to Dimitri Mantheakis (Lithos Africa, Dar es Salaam, Tanzania), and also to the Saul family (Swala Gem Traders, Arusha, Tanzania) and Tanzanian broker Abdul Msellem for their assistance in arranging our trips to the Winza mining area. Some preliminary observations from our visits are reported here, and further information is in preparation for an article that we plan to submit to *Gems & Gemology*.

The mining area is located approximately 10 km southwest of the village of Winza, and can be reached by four-



Figure 34. These ruby crystals from Winza display rhombohedral and prismatic habits. Some stones contain blue patches in crystallographically defined zones. The largest crystal is 25 mm wide and weighs 17.6 g. Photo by H. A. Hänni, © SSEF.



Figure 35. Bent needles, such as these seen in one of the rough Winza rubies (left, magnified 30×), were also present in the 10.75 ct faceted ruby examined at BaselWorld and appear to be characteristic of material from this locality. The partially healed fissure on the right (magnified 20×) consists of multiphase inclusions, which were also commonly seen in the rough Winza rubies and the faceted stones examined at BaselWorld. Photomicrographs by H. A. Hänni, © SSEF.

wheel-drive vehicle in about 2½ hours (much longer during the wettest season, in March-April) from the nearest small town, Mpwapwa. At least 5,000 miners have rushed to the deposit and are using hand tools to excavate shallow pits in eluvial soil (figure 36). The excavated material is loaded into sacks, carts, or trucks, and brought to the nearby stream for washing. There, the soil is wet-screened and the gems are removed by hand (figure 37). In addition, several shafts have been dug by hand to depths reaching 30 m to explore the underlying hard-rock deposits. The corundum occurs within a dark, fine-grained metamorphic host rock, as aggregates and isolated crystals that are well formed and typically color zoned (e.g., with an irregular dark blue surface layer and a pink-to-red interior). Raman analysis of a piece of corundum-bearing host rock by GIA Laboratory staff gemologist Karen M. Chadwick showed that it is composed of amphibole (and is therefore an amphibolite), and locally contains irregular areas of brown garnet that are associated with the corundum.

It appears that most of the ruby and sapphire from Winza has come from the eluvial workings. There was no evidence that any corundum has been produced from the alluvium within the stream where the material is washed. However, in one of the corundum parcels we saw gem-quality pieces of a waterworn pinkish orange mineral represented as garnet, which were reportedly recovered from the same area.

Most of the ruby and sapphire production is being routed to dozens of Thai and Sri Lankan (and a few African) buying offices in Mpwapwa. The material we were shown in Mpwapwa consisted mostly of lower-quality fragments, in a range of colors (often zoned) from blue to violet, purple (rarely), pink, and red. Due to the informal nature of the mining, it was impossible to determine how much corundum was being produced, but we estimate that at the times

of our visits the miners were gathering a few kilograms per day of mixed-quality material. By early June, however, the water in the stream had grown scarce, resulting in a corresponding decrease in production (D. Mantheakis, pers. comm., 2008). So far, gem corundum from Winza has been recovered from an area measuring several square kilometers, but the overall size of the deposit is not yet known.

Brendan M. Laurs  
Vincent Pardieu  
Gübelin Gem Lab  
Lucerne, Switzerland

Figure 36. Miners use picks and shovels to excavate shallow pits in search of ruby and sapphire at Winza, Tanzania. Photo by V. Pardieu.





Figure 37. The eluvial soils are brought to the nearby river for washing, screening, and hand-picking of the ruby and sapphire. Photos by B. M. Laurs.

**A sapphire with *en echelon* inclusions.** Sapphire, whether natural or treated, exhibits a wide range of inclusion features. In addition to their diagnostic value, these features often provide gemologists with interesting imagery. One such sapphire was examined recently at the Gem Testing Laboratory of Jaipur.

The RI and SG of the 11.31 ct light violetish blue mixed-cut oval (figure 38) were consistent with those of natural or synthetic sapphire. There was no reaction to long- or short-wave UV radiation, and no absorptions were seen with the desk-model spectroscope. When examined with magnification, the stone displayed some linear whitish zones of dotted inclusions, which are commonly associated with natural sapphire (heated or unheated). At higher magnification, these zones appeared to be com-

Figure 38. This 11.31 ct sapphire contains some distinctive inclusions. Photo by G. Choudhary.



posed of fine white pinpoints arranged *en echelon* (i.e., as subparallel overlapping or step-like features; see figure 39). We could not determine the exact orientation of these linear zones relative to the c-axis, but the optic axis was inclined to the planes containing these features. Hence, we can only speculate that the dotted inclusions were oriented along the dipyrnidal faces of the crystal. Although these features did not indicate whether the sapphire had been heated, they offered conclusive proof that the stone was of natural origin, as such inclusions have not been reported in synthetic sapphires.

Other inclusions observed in this sapphire were a “burst halo” centered around a white sugary crystal (figure 40, left) and numerous surface-reaching fingerprint-like

Figure 39. At relatively high magnification, linear trains of *en echelon* inclusions were visible in the sapphire. Photomicrograph by G. Choudhary; magnified 85 $\times$ .





Figure 40. The presence in corundum of a white, sugary crystal with an associated stress fracture (left) is typically associated with high-temperature heat treatment. Surface-reaching fingerprint-like inclusions (right) are further evidence of heat treatment. Photomicrographs by G. Choudhary; magnified 80× (left) and 60× (right).

inclusions (figure 40, right), both of which are commonly seen in corundum that has been exposed to high-temperature heating. The latter features are essentially surface breaks into which some foreign substance (e.g., borax) penetrated the stone during heat treatment.

The exact nature of the *en echelon* inclusions could not be determined. However, our observations of the overall inclusion features led us to identify the sapphire as natural with “indications of heat treatment.”

Gagan Choudhary

**Serpentinite artifact resembling Libyan desert glass.** In February 2008, the SSEF Swiss Gemmological Institute received an unusual object (figure 41) that was found at an archeological site in the Lop Nur dry lake bed in the Taklamakan Desert of Xinjiang Province, northwestern China. According to Dr. Christoph Baumer, a Swiss archeologist who worked on the excavation, the artifact was reportedly discovered near a 2,000-year-old jade axe.

The translucent yellow bar (56.02 ct) had a distinctly worked outline. One end was rounded while the other was irregular, suggesting that it had been broken in the past. Visually, the item resembled natural desert glass from Libya. The heavily etched surface was similar to that com-

monly seen on desert glasses, which have typically been exposed to prolonged abrasion by sand storms (figure 42). However, the uniform shape strongly suggested a manufactured object.

Standard gemological testing was inconclusive: hydrostatic SG—2.59; fluorescence—slightly yellow to long-wave UV radiation and no reaction to short-wave UV; handheld spectroscope—no absorption seen; polariscope reaction—always bright, indicating an anisotropic aggregate. Due to the irregular surface, no refractive index could be measured.

As a next step, the chemical composition of the item was qualitatively determined by EDXRF spectroscopy. In contrast to Libyan desert glass, which is nearly pure silica glass with some minor amounts of Fe and other trace elements, this specimen showed both Si and Mg as main constituents; minor amounts of Fe were also detected. Based on the chemical composition and the appearance between crossed polarizers, it was evident that the material was not a glass but rather a polycrystalline aggregate of a Mg-silicate such as antigorite (serpentine group). The Raman spectrum confirmed this identification, with four distinct peaks at 1045, 688, 377, and 231  $\text{cm}^{-1}$ , which matched our reference spectrum for antigorite. In the gem trade, translucent light yellow antigorite is known as *bowenite serpentine*.

Figure 41. This unusual artifact (39.3 × 18.3 × 6.8 mm), which was discovered at an archeological site in the Taklamakan Desert of China's Xinjiang Province, proved to be antigorite (bowenite serpentine). Photo by H. A. Hänni, © SSEF.

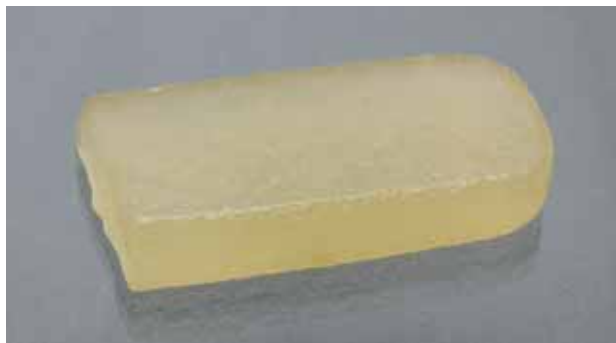


Figure 42. The serpentinite artifact's irregular surface etching is likely due to prolonged abrasion by wind-blown desert sands, as is often seen in desert glasses. Photo by H. A. Hänni, © SSEF.



As antigorite is relatively soft (5.5 on the Mohs scale), it has long been used for jewelry and carving purposes, especially in China (see R. Webster, *Gems*, 5th ed., revised by P. G. Read, Butterworth-Heinemann, Oxford, UK, 1994, pp. 275–276). The etched surface of the broken end indicated that it had been broken before it was exposed to prolonged abrasion in the dry and windy climate of the Taklamakan Desert.

Michael S. Krzemnicki (*gemlab@ssef.ch*)  
SSEF Swiss Gemmological Institute  
Basel, Switzerland

**Star and cat's-eye topaz from Brazil.** Topaz is a common gem, but only rarely does it occur with chatoyancy or asterism. The largest cat's-eye topaz described in the literature thus far was a 270 ct stone from Ukraine (Winter 2004 GNI, p. 346); star topaz has not been previously reported. However, in August 2005 this contributor acquired a star topaz in Brazil, and it was even larger than the 270 ct cat's-eye stone.

The egg-like cabochon (figure 43) weighed 333.27 ct and measured 38.2 × 33.5 × 28.0 mm. It was identified as topaz by standard gemmological methods. The stone was filled with semiparallel flat, hollow channels, similar to a pale blue 152.15 ct cat's-eye topaz from Brazil that this contributor also described (figure 44; J. Hyršl, "Some new unusual cat's eyes and star stones," *Journal of Gemmology*, Vol. 27, No. 8, 2001, pp. 456–460).

The channels were much more common in one half of

Figure 44. This cat's-eye topaz (152.15 ct), also from Brazil, shows chatoyancy resulting from internal features similar to those causing the asterism in the stone in figure 43. Photo by J. Hyršl.

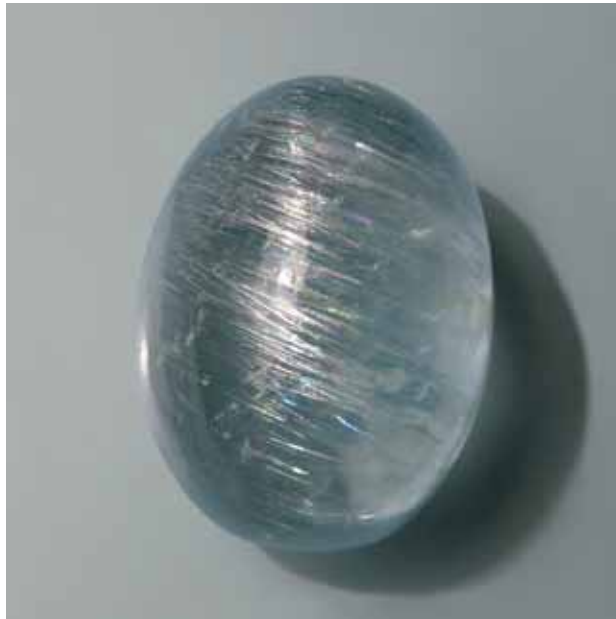
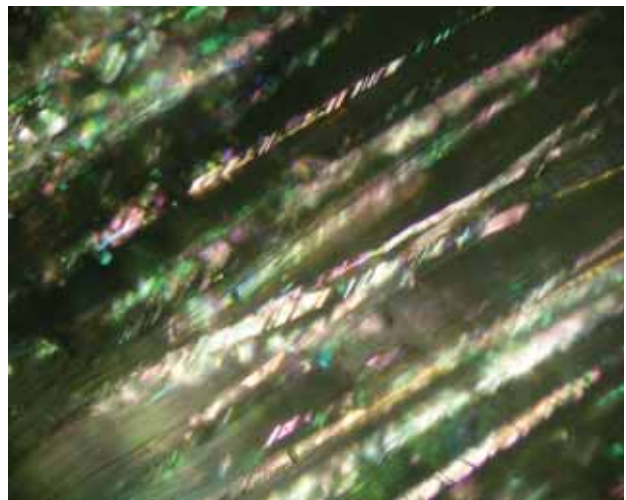


Figure 43. This extremely rare star topaz from Brazil (333.27 ct) shows asterism—composed of a vertical yellow ray and a white ray oriented at about 40° to the yellow ray—that is caused by oriented growth tubes and internal striations within the tubes. Photo by J. Hyršl.

the stone, and the border between the two halves was sharp, confirming that the tubes were the result of a growth phenomenon, not etching. The stone showed two rays when illuminated with a strong spotlight (again, see figure 43). One ray was yellow and oriented perpendicular to the hollow channels. The second ray was white and oriented at an angle of about 40° from the first ray; with magnification, it showed bright iridescent colors (figure 45). The cause of the second ray was apparent only with high magnification: The channels were not smooth inside, but rather showed strong striations at an angle of

Figure 45. Striations on the inner surface of the sub-parallel hollow channels are the cause of the reflective white ray in the star topaz. Photomicrograph by J. Hyršl, reflected light; field of view 2 mm.



about 40° to their length. Similar striations in topaz were reported by J. I. Koivula more than 20 years ago (see figure 6 in “The rutilated topaz misnomer,” Summer 1987 *Gems & Gemology*, pp. 100–103). These striations were responsible for the asterism in the 333 ct topaz and the cat’s-eye effect in the 152 ct topaz. Both are likely from the same locality, said to be alluvial cassiterite deposits in the state of Rondônia.

It is interesting to note that there exists a third possible cause of chatoyancy in topaz, which was described by W. Kumaratilake (“Gems of Sri Lanka: A list of cat’s eyes and stars,” *Journal of Gemmology*, Vol. 25, No. 7, 1997, pp. 474–482). According to this report, chatoyancy in white topaz from Sri Lanka is caused by parallel blade-like sillimanite inclusions. Compared to the stones from Brazil, cat’s-eye topaz from Sri Lanka (e.g., figure 46) is much more transparent, the internal chatoyancy-causing features are very fine, and the eye is sharper.

Jaroslav Hyršl (hyrsl@kuryr.cz)  
Prague, Czech Republic

**A new source of Persian turquoise: Kerman, Iran.** The Iranian Neyshabur mines in Khorasan Province have historically been known for producing the finest Persian turquoise. However, in recent years these deposits have not yielded much high-quality material. In 2005, a new turquoise area was discovered in Kerman Province, 1,200 km southwest of the Neyshabur mines. This new mining area is located approximately 90 km northeast of the town of Bardsir (Mashiz), at 30°03’ N and 56°30’ E. The mine is

Figure 46. In this cat’s-eye topaz from Sri Lanka (28.24 ct), the chatoyancy is caused by oriented sillimanite inclusions. Photo by J. Hyršl.



Figure 47. A new source of turquoise has been discovered near Bardsir in Kerman Province, Iran. The three cabochons and two partially polished pieces (9.49–29.79 ct) were characterized. Photo by Robert Weldon.

owned by local people from Kerman City, who employ about eight workers and use an excavator. The turquoise was found accidentally while they were searching for copper. Summers in this region are dry with daytime temperatures typically over 38°C (100°F), while winters are rainy with occasional snowstorms.

Approximately 800–1,000 kg of mixed-quality turquoise (including porous chalky material) was recovered in the 2007–2008 mining season (starting in June–September and going until December). The color range is similar to that from the Neyshabur mines, varying from very light blue to “sky” blue (e.g., figure 47). Some dark greenish blue to yellowish green material has also been recovered. As much as 5% of the total production is high-quality “sky” blue material, which is usually found in small sizes ranging from 1 to 5 cm (although larger pieces have been recovered; see, e.g., figure 48).

The geology of this area is similar to that at Neyshabur. The turquoise is hosted by a deeply weathered porphyritic volcanic rock (trachyte) that contains phenocrysts of alkali feldspar and quartz, and is locally cemented by limonite (all minerals identified solely by visual means).

One piece of rough, two partially polished pieces, and three cabochons of the Bardsir turquoise were loaned to



Figure 48. Some large pieces of high-quality turquoise (here, 12 × 7 cm) have been recovered from the Bardsir deposit. Photo by M. Douman.

GIA for examination (again, see figure 47). One of us (EAF) determined the following properties on the five polished stones: color—greenish blue, with no pleochroism; spot RI—1.61–1.62; hydrostatic SG—2.65–2.75; Chelsea filter reaction—none; fluorescence—weak blue to long-wave and inert to short-wave UV radiation; and an absorption band at 430 nm visible with the desk-model spectroscope. These properties are consistent with those reported for turquoise by M. O'Donoghue, Ed. (*Gems*, 6th ed., Butterworth-Heinemann, Oxford, UK, 2006, pp. 323–328). Microscopic examination revealed inclusions of quartz, pyrite, and chalcopyrite, all identified by Raman analysis.

The higher-quality material from this new deposit does not need any treatment, and the availability of some pieces in rather large sizes is also encouraging.

Makhmout Douman ([makhmout@arzawa.com](mailto:makhmout@arzawa.com))  
 Arzawa Mineralogical Inc., New York

Eric A. Fritz  
 Denver, Colorado

**A rare faceted yellow vanadinite.** Vanadinite  $[Pb_5(VO_4)_3Cl]$  is an uncommon mineral found in arid climates that forms as a result of the oxidation of primary lead minerals (W. L. Roberts et al., Eds., *Encyclopedia of Minerals*, Van Nostrand Reinhold, New York, 1974, p. 646). Faceted

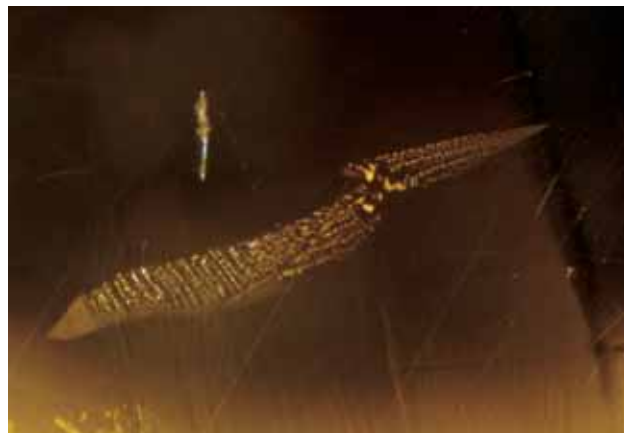


Figure 49. This extremely rare 2.40 ct vanadinite was cut from material reportedly recovered from a new surface prospect located in the DRC. Photo by Robert Weldon.

vanadinite is extremely rare. However, gem dealer Mark Kaufman recently loaned a 2.40 ct bright yellow round modified brilliant vanadinite (figure 49) to GIA for study. He cut the stone from rough material supplied by Dr. Rob Lavinsky (The Arkenstone, Garland, Texas), who reported that it came from a new surface prospect at an undisclosed locality in the Democratic Republic of the Congo (DRC).

The faceted vanadinite yielded the following properties: color—highly saturated yellow; RI—over the limit of the refractometer; birefringence—high, as evidenced by the strong doubling of the crown facet edges when viewed through the pavilion; hydrostatic SG—7.24; fluorescence—weak orange-red to long- and short-wave UV radiation. No absorption features were observed with the desk-model spectroscope. With the exception of the bright yellow color,

Figure 50. The faceted vanadinite contained a healed fissure consisting of minute particles in parallel formations. Photomicrograph by R. Befi; image width 1.0 mm.



these properties are consistent with those reported for vanadinite by Roberts et al. (1974).

The faceted stone was transparent, with only a few inclusions. Microscopic examination showed two small “fingerprints” (see, e.g., figure 50) and long, thin growth tubes intersecting tiny flat inclusions. No growth banding or color zoning was observed. The girdle was chipped; the crown, table, and pavilion showed abrasions and scratches; and the facet edges were rounded rather than sharp. This was consistent with vanadinite’s low hardness (2½–3 on the Mohs scale) and brittleness.

The chemical composition of the faceted stone (determined by EDXRF) was also consistent with vanadinite, with major amounts of Pb and V. The Raman spectrum, taken with 514 nm laser excitation, consisted of peaks at 828, 356, and ~324  $\text{cm}^{-1}$ , matching our vanadinite reference. The UV-Vis-NIR absorption spectra showed that the ordinary ray and extraordinary ray had similar absorption peaks at 589, 754, and 807 nm.

Vanadinite is known from several localities, including the U.S., Mexico, Scotland, Sardinia, Austria, Russia, Algeria, Tunisia, and Morocco. To the best of this contributor’s knowledge, this is the first report of vanadinite from the DRC. In addition, this is believed to be the first faceted vanadinite examined at the GIA Laboratory.

Riccardo Befi ([riccardo.befi@gia.edu](mailto:riccardo.befi@gia.edu))  
GIA Laboratory, New York

## SYNTHETICS AND SIMULANTS

**Experimental CVD synthetic diamonds from LIMHP.** The SSEF Swiss Gemmological Institute recently studied two near-colorless (slightly gray; figure 51) slices of synthetic diamond grown by chemical vapor deposition (CVD) at the Laboratoire d’Ingénierie des Matériaux et des Hautes Pressions (LIMHP) in Paris. One sample ( $4.15 \times 3.70 \times 0.20$  mm, 0.05 ct), referred to here as sample A, showed features typical of CVD synthetic diamond (P. M. Martineau et al., “Identification of synthetic diamond grown using chemical vapor deposition [CVD],” Spring 2004 *Gems & Gemology*, pp. 2–25). However, the other slice ( $4.01 \times 3.99 \times 0.35$  mm, 0.09 ct; sample B) showed features that were quite distinct from those of previous CVD synthetic diamonds grown at LIMHP, which were described by W. Wang et al. (“Experimental CVD synthetic diamonds from LIMHP-CNRS, France,” Fall 2005 *Gems & Gemology*, pp. 234–244).

Observed between crossed polarizing filters, the two samples showed very different reactions: Sample A displayed considerable strain, similar to the cross-hatched “tatami” patterns observed in natural type II diamonds, while sample B was nearly strain free. Microscopic examination revealed the presence of very small whitish and roundish inclusions in both samples.

In contrast to earlier reports, in which orange-red fluorescence was commonly observed in CVD synthetic diamonds (see, e.g., P. M. Martineau et al., 2004), both slices

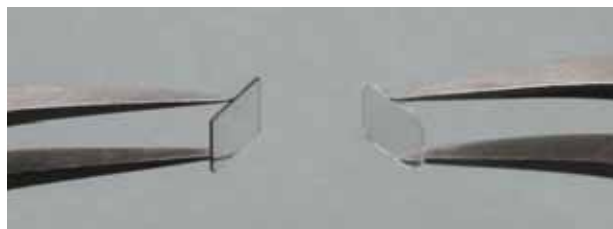


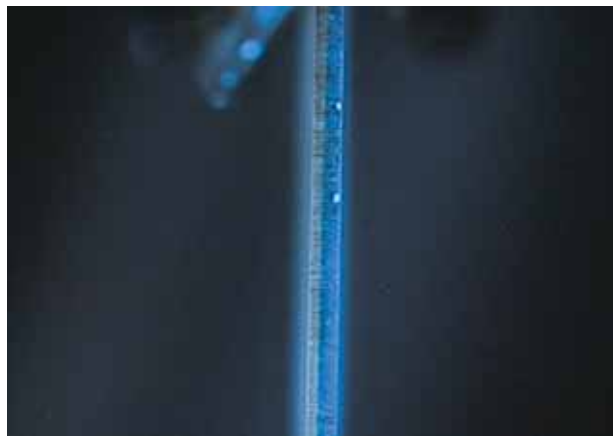
Figure 51. These thin slices of CVD synthetic diamonds (~4 × 4 mm) were grown by LIMHP in Paris. Sample A is shown on the left, and B is on the right. Photo by L. Phan, © SSEF.

were inert to long- and short-wave UV radiation, similar to the more recent samples described by W. Wang et al. (“Latest-generation CVD-grown synthetic diamonds from Apollo Diamond Inc.,” Winter 2007 *Gems & Gemology*, pp. 294–312). Examination with the DiamondView instrument revealed two parallel zones in sample A when observed from the side, due to growth in layers (figure 52), which is typical for the CVD process. One zone had a bluish reaction and the other zone was inert. Sample B was entirely inert.

FTIR spectroscopy showed no nitrogen or boron above the detection limit in either sample, classifying them as type IIa. However, sample A showed two large bands centered at 4723 and 4659  $\text{cm}^{-1}$ , which have not been previously reported. The UV-Vis-NIR spectra (200–1800 nm) of both samples matched those of near-colorless type IIa diamonds, with no absorption features except a weak progressive absorption from 450 nm to a cutoff at 225 nm.

The photoluminescence spectra, recorded at liquid-nitrogen temperature (77 K) with a 514 nm laser source, were very interesting. Sample B showed only the intrinsic diamond Raman peak at 1332  $\text{cm}^{-1}$ ; the Si-V center, usually present at about 737 nm, was notable by its absence.

Figure 52. Sample A, when observed from the side in the DiamondView instrument, shows two different fluorescence zones, a sign of growth in layers. Photo by P. Lefèvre, © SSEF.



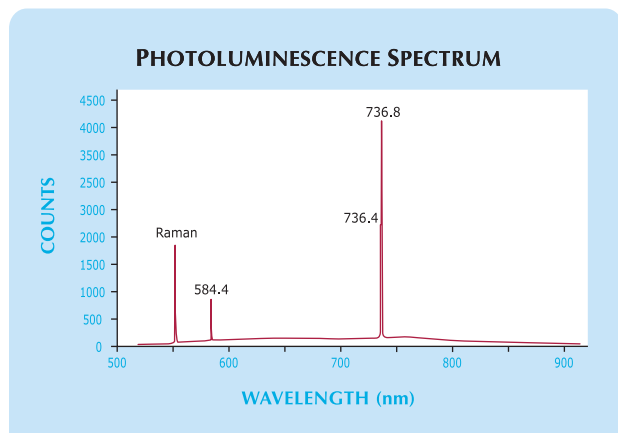


Figure 53. The photoluminescence spectrum of CVD synthetic diamond sample A shows a doublet at 736.4 and 736.8 nm, characteristic of Si-V centers.

This matches results obtained by Martineau et al. (2004) for CVD synthetic diamond grown by Element Six and by Wang et al. (2007) for samples provided by Apollo Diamond, which also did not show this defect. The PL spectrum of sample A (figure 53) showed peaks at 584.4, 736.4, and 736.8 nm; the latter two formed a doublet that is characteristic of Si-V centers.

These two samples were interesting because, although they were grown in the same plasma reactor, different experimental parameters (F. Silva, LIMHP, pers. comm., 2007) led to completely different characteristics. Sample A was relatively easy to identify as CVD synthetic diamond using the DiamondView and PL spectroscopy. The other sample was more difficult, because it did not show the typical growth and spectroscopic characteristics, especially Si-V centers in its PL spectrum at 514 nm excitation. (However, it is possible that Si-V centers could have been resolved using 633 nm excitation, but this was not available on our instrument.) Additionally, both stones lacked

Figure 54. This 30.12 ct piece of faceted glass was sold as rubellite. The elongated straight lines are gas bubbles. Photo by B. Mocquet.



the orange-red UV fluorescence that previously aided identification by gemological testing.

These two samples were too thin to be cut into gemstones, but larger samples may be grown in the future that lack the typical features of CVD synthetic diamonds, similar to sample B, and these could present significant identification challenges.

Pierre Lefèvre and Jean-Pierre Chalain (gemlab@ssef.ch)  
SSEF Swiss Gemmological Institute  
Basel, Switzerland

**Unusual glass imitation of rubellite.** We recently examined a 30.12 ct gem that had been sold as rubellite in Jaipur, India. When observed face-up, it convincingly resembled a color-zoned rubellite (figure 54). When observed perpendicular to its width, however, the specimen had a very uneven coloration, with alternating colorless and vivid pink cylinders (figure 55). The sample was singly refractive (1.47 RI) and had a hydrostatic SG of 2.51. It was inert to long-wave UV radiation and fluoresced strong chalky blue to short-wave UV. With the microscope, one could see elongated bubbles parallel to the colored cylinders. In some cases, the bubbles were so elongated that they reached both sides of the faceted stone, mimicking growth channels. All these gemological properties were consistent with a manufactured glass.

To determine the exact composition of this glass and look for possible variations between the pink and colorless zones, we analyzed its chemical composition with a JEOL 5800 scanning electron microscope equipped with a high-resolution Princeton Gamma Tech IMIX-PTS germanium energy-dispersive detector. The instrument was operated

Figure 55. This side view of the sample reveals that the glass is made up of successive colorless and vivid pink cylindrical layers. Photo by B. Mocquet.



using an accelerating voltage of 20 kV, a current of 1 nA, and a 37° take-off angle. The composition was consistent with a glass, containing 78.0% SiO<sub>2</sub>, 4.3% K<sub>2</sub>O, 2.5% CaO, 9.7% Na<sub>2</sub>O, 1.0% Al<sub>2</sub>O<sub>3</sub>, 1.0% BaO, 0.6% ZnO, 0.5% MgO, and 0.2% FeO (values expressed in wt.%). We did not detect any systematic chemical differences between the pink and colorless zones.

To understand the origin of the pink color, we measured the UV-Vis absorption spectrum of this glass with a Unicam UV4 spectrophotometer in the 350–800 nm range. The main spectral features were a broad band centered at ~540 nm and a continuum of absorption regularly increasing from the red to the UV region. A similar broad band has been observed in “ruby glass” of equivalent color (Jean-Pierre Razmoket, pers. comm., 2008). Therefore, the coloration was likely due to Mie scattering on submicroscopic metallic inclusions of either gold or copper (G. Mie, “Beiträge zur Optik trüber Medien, speziell kolloidaler Metallösungen [Contributions to optics, opaque media, especially metal colloidal solutions],” *Annalen der Physik*, Vol. 4, No. 25, 1908, pp. 377–445). We could not observe these features using the SEM because they are likely smaller than the resolution of our instrument.

This type of material, in particular the pink central cylinders, is not unlike Venetian glass, widely used for centuries as man-made jewels or gem imitations.

*Benjamin Rondeau, Emmanuel Fritsch,  
Yves Lulzac, and Blanca Mocquet*

**Tourmalines and their imitations obtained in Kandahar, Afghanistan.** Matthew McCann, stationed with the American forces in Kandahar, Afghanistan, purchased five gems represented as tourmalines (figure 56) in the local bazaar. He suspected that the two largest of these (10.58 and 11.35 ct) were fake, because of their relatively large sizes combined with the fact that they were eye-clean and bicolored in unusual hue combinations for tourmaline: purple/near colorless and yellow/green. Mr. McCann sent all five samples to the University of Nantes for analysis.

When observed from the side, the large yellow/green emerald cut displayed a planar colorless zone a little over 1 mm thick, with parallel yellow zones on both sides that

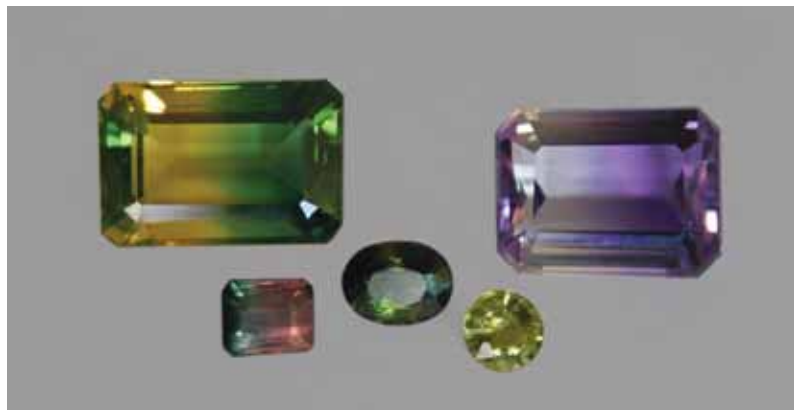


*Figure 56. These five gems were sold as tourmalines in a bazaar in Kandahar, Afghanistan. The two larger emerald cuts proved to be quartz, one natural (purple/near colorless, 10.58 ct) and one synthetic (yellow/green, 11.35 ct). Photo by Alain Cossard.*

were 3–4 mm thick (figure 57, left). Green zones flanked the yellow areas (although only one green zone is shown in figure 57, left). A series of purple and near-colorless lamellae were visible across the width of the pavilion in the other large emerald cut (figure 57, right).

Both samples had RIs of 1.54–1.55, a hydrostatic SG of 2.65, no luminescence to UV radiation, and were uniaxial positive. These properties identified them as quartz rather than tourmaline. Neither sample showed twinning, and in both the optic axis was roughly parallel to the table. In addition, the colorless zone in the yellow/green emerald cut was perfectly planar, with minute inclusions bordering it on both sides, corresponding to the seed plate in synthetic quartz. The purple/near-colorless zoning of the other large stone indicated that it was a natural amethyst, as such zoning is known in natural quartz but has not been reported in synthetic quartz.

The other three stones—a dark green 1.42 ct oval, a slightly greenish yellow 0.64 ct round, and a 1.33 ct bicolored green-pink emerald cut (again, see figure 56)—proved to be tourmalines, as indicated by their RIs of about 1.62–1.64, SG of ~3.05, and uniaxial negative optic character. The last two stones actually appeared biaxial on the refractometer

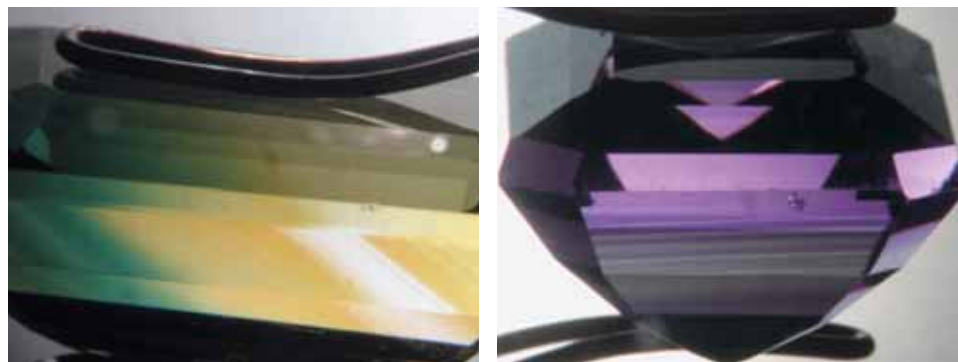


*Figure 57. Symmetrical yellow and green zoning ran parallel to a colorless seed plate in the 11.35 ct synthetic quartz (left); note the pinpoint inclusions near the seed. The sharp, fine, parallel-planar zoning seen in the 10.58 ct purple/near-colorless quartz (right) has not been reported in synthetic amethyst. Photomicrographs by E. Fritsch.*

(i.e.,  $n_o = 1.633\text{--}1.641$  and  $n_e = 1.618\text{--}1.628$  for the greenish yellow stone;  $n_o = 1.635\text{--}1.640$  and  $n_e = 1.620\text{--}1.640$  for the bicolored tourmaline), but uniaxial with the conoscope (the optic figure in the bicolored stone could only be seen with immersion in heavy liquid). This somewhat unusual behavior might be explained in part by internal stress, which was visible between crossed polarizers as a “tatami” pattern.

This is a good example of synthetic stones being used as imitations of yet another gem variety. Also, it reinforces the fact that even buying stones close to the source can be problematic without some basic identification equipment.

*Emmanuel Fritsch, Yves Lulzac,  
and Benjamin Rondeau*

## CONFERENCE REPORTS

**Sinkankas Garnet Symposium.** The sixth annual symposium in honor of John Sinkankas took place April 19, 2008, at GIA in Carlsbad. Co-hosted by GIA and the San Diego Mineral and Gem Society, the sold-out event had 148 people in attendance.

After opening remarks by convener Roger Merk (Merk’s Jade, San Diego, California), **Lisbet Thoresen** (Beverly Hills, California) reviewed the use of gem materials (including garnet) by Bronze Age and Classical cultures. She noted that the following inclusions have been documented within garnets set in ancient objects: rutile needles, apatite, metamict zircon, monazite with tension halos, and possibly ilmenite. **Dr. William “Skip” Simmons** (University of New Orleans) covered the mineralogy and crystallography of the garnet group. Of the 15 garnet species recognized by the International Mineralogical Association, only four (pyrope, almandine, spessartine, and grossular) are important gem materials. **Si Frazier** (El Cerrito, California) reviewed the history and lore of garnets. He noted that lapidaries used heavy steel weights to break almandine garnet from western Europe, with the resulting tabular pieces aptly suited for carvings or gem inlay. **William Larson** (Pala International, Fallbrook, California) reviewed the sources and mining for Russian demantoid. Within the past two years, several small alluvial deposits have been discovered in the Ural Mountains near the historic mines.

**Meg Berry** (Mega Gem, Fallbrook, California) illustrated the faceting and carving of garnet, showing how the appearance of overdark rhodolite can be lightened by cutting a 40° facet at each corner, and describing the successful carving of large pieces of spessartine (80 and 137 ct) into free-form designs. **Robert Weldon** (GIA, Carlsbad) provided suggestions for getting the best photos of garnets—applicable to other gems as well—including the use of light backgrounds for dark stones (and vice versa) and diffused lighting to avoid hot spots (with the exception of capturing the phenomenon in iridescent garnets, which are best photographed using a fiber-optic light source). **Dr. William Hanneman** (Hanneman Gemological Instruments, Rio Rancho, New Mexico) discussed garnet nomenclature, and stressed the importance of correlating any new garnet trade

names with their proper mineralogical equivalent.

**John Koivula** (GIA, Carlsbad) reviewed the wide variety of internal features found in garnet (e.g., growth zoning, strain, and inclusions such as sulfides, rutile, Cr-diopside, and forsterite), and also the occurrence of garnet as an inclusion in other minerals (e.g., spessartine in quartz, chrysoberyl, topaz, beryl, and obsidian). **Dr. George Rossman** (California Institute of Technology, Pasadena) reviewed the primary causes of color in garnets, which relate to  $\text{Fe}^{2+}$ ,  $\text{Fe}^{3+}$ ,  $\text{Cr}^{3+}$ ,  $\text{V}^{3+}$ ,  $\text{Mn}^{2+}$ , and  $\text{Mn}^{3+}$ , as well as  $\text{Fe}^{2+}\text{-Ti}^{4+}$  interactions.

The theme of next year’s Sinkankas Symposium (date to be determined) will be spinel.

*Brendan M. Laurs*

**2008 Scottish Gemmological Association conference.** This conference, held May 2–5 at The Queens Hotel in Perth, Scotland, featured a variety of topics.

**Dr. George Rossman** (California Institute of Technology, Pasadena) delivered two talks. The first described his latest research on nanoscale features in minerals that relate to origin of color and optical phenomena. These included the cause of asterism in rose quartz (which is due to nanofibers of a new mineral related to dumortierite), star almandine from Idaho (minute hollow tubes), and star corundum (rutile in Sri Lanka and diasporite in Tanzanian material). Dr. Rossman’s second talk focused on historic and modern technologies for modifying color in gem materials (beryl, zircon, corundum, amethyst, and tourmaline), and the current understanding of the atomic processes involved in such treatments.

**David Callaghan** (London), formerly senior director of the estate jeweler Hancocks, offered insight into jewelry from the Art Deco period leading up to the abdication of Edward VIII, and reviewed various pieces the monarch gave to the Duchess of Windsor. In particular, he described her flamingo and panther brooches, and also her charm bracelet consisting of gemstone crosses that the duke had engraved with secret messages for special occasions.

**Alan Hodgkinson** (Ayrshire, Scotland), the Association’s president, presented methodology for “top-lighting the refractometer,” in which a light beam is passed vertically down through the stone placed on the hemicylinder. He also reviewed techniques for dealing with tiny stones and uneven cabochon surfaces, and described the ideal amount of liquid used for the spot RI method.

**Elisabeth Strack** (Gemmological Institute of Hamburg, Germany) discussed the results of her testing of the emeralds in Mogul objects from the Gold Room at the Hermitage State Museum in St. Petersburg, Russia, which date from the 16th century. She concluded that the emeralds were Colombian, given the fact that they contained jagged three-phase inclusions. She also detected oil residue in fissures and fractures. Her tests were performed using only limited gemological techniques since she did not have access to advanced instrumentation in the museum.

**Stephen Whittaker** (Fellows and Sons Auctioneers,

Birmingham, UK) reviewed the wide variety of interesting and unusual items that have recently passed through the auction house. Some of the items received far more attention and higher bids than anticipated due to publicity.

In addition to the keynote talks, several short presentations were delivered. **Brian Jackson** (National Museum of Scotland, Edinburgh) discussed strong yellow and blue pleochroism in apatite from Lake Baikal, Russia. **Harold Killingback** (independent gemologist) explored asterism in rose quartz using a red laser pointer and some reflectors. **Anton Vasiliev** (LAL, Moscow, Russia) described how his Facet Design Software helps plan and predict the result of cutting colored stones by accounting for the lighting, transparency, RI, and proportions.

Rounding out the event were several workshops, on "Emerald Inclusions," "Spectra of Red Stones," "Facet Design Software," "Opals," "Filters," and "Auction Items," as well as a post-conference field trip to collect an ornamental stone called haggis rock from the Peebles area of Scotland. The group also visited Lauriston Castle to see the famous Blue John collection.

*Cigdem Lule-Whipp (cigdem@gialondon.co.uk)  
GIA London*

## ANNOUNCEMENTS

**CIBJO introduces *Precious Metals Blue Book*.** CIBJO, the World Jewellery Confederation, recently launched the first edition of its *Precious Metals Blue Book*. This publication, aimed at ensuring consumer confidence and promoting best practices, provides standards for precious metal alloys, finenesses, weights, colors, tolerances, solders, coatings/platings, and markings. It covers precious metal jewelry, flatware, and hollowware. The manual will soon be available in electronic format on the CIBJO website, [www.cibjo.org](http://www.cibjo.org).

### Conferences

**IGC 2008.** Held in Oslo, Norway, on August 6–14, the *33rd International Geological Congress* will include sessions with possible applications to gemology: mineral spectroscopy; metallogeny and mineral potential of Russia, Belarus, and Ukraine; geology of Africa; and development strategies for the mining sectors of African countries. Visit [www.33igc.org](http://www.33igc.org).

**9th International Kimberlite Conference.** Held August 10–15, 2008, in Frankfurt, Germany, this conference will bring together the academic and diamond exploration communities to exchange information on kimberlites, related rocks, and diamonds. Visit [www.9ikc.com](http://www.9ikc.com).

**WJA "Women in the Know" conference.** The Women's Jewelry Association will host its second annual West Coast "Women in the Know" conference August 15, 2008, in Los Angeles. It will include presentations on leadership skills, entrepreneurship, luxury marketing strategies, jew-

elry manufacturing, and more. The conference will directly precede the West Coast Jewelry Show, which runs August 16–18. Visit [www.womensjewelry.org](http://www.womensjewelry.org).

**IUCr2008.** Crystal growth, characterization, and analytical techniques will be covered at the *21st Congress and General Assembly of the International Union of Crystallography*, held in Osaka, Japan, August 23–31. Visit [www.congr2008.co.jp/iucr2008](http://www.congr2008.co.jp/iucr2008).

**FIPP 2008 gem show and mine tour.** The International Gem Fair known as FIPP (Feira Internacional de Pedras Preciosas) will take place in Teófilo Otoni (Minas Gerais, Brazil) August 26–30, 2008. Following the show, a 10-day tour will visit various gem deposits in Minas Gerais. There will be an optional four-day extension to the amethyst mines of Rio Grande do Sul State. Visit <http://customgroup.travel/brazil/tour.htm>. An 11-day Brazilian gem tour can also be scheduled through [www.tourguidebrazil.com/mineraltour.html](http://www.tourguidebrazil.com/mineraltour.html).

**6th International Conference on Mineralogy and Museums.** Held September 7–9, 2008, at the Colorado School of Mines, Golden, Colorado, conference themes are the relationships between museums and research, collection management, and society. Gems will form a significant part of the program, and pre- and post-conference field trips are being planned to kimberlite and pegmatite sites in Colorado. Visit [www.mines.edu/outreach/cont\\_ed/ICMM6](http://www.mines.edu/outreach/cont_ed/ICMM6).

**Diamond 2008.** The *19th European Conference on Diamond, Diamond-like Materials, Carbon Nanotubes, and Nitrides* will be held in Sitges, Spain, September 7–11. Program topics include the growth, processing, and characterization of diamond. Visit [www.diamond-conference.elsevier.com](http://www.diamond-conference.elsevier.com).

**Rapaport International Diamond Conference.** Taking place September 8, 2008, in New York, this conference will cover diamond finance, rough supply, manufacturing, commoditization, and fair trade jewelry. E-mail [IDC@diamonds.net](mailto:IDC@diamonds.net).

**ICAM 2008.** Gems will be one of the subjects covered at the *9th International Congress for Applied Mineralogy*, held September 8–10 in Brisbane, Australia. Visit [www.icam2008.com](http://www.icam2008.com).

**World of Gems.** The inaugural session of this conference, addressing current developments in gem treatments, identification, diamond grading, and appraisal issues, will be held September 13–14, 2008, in Chicago, Illinois. Visit [www.worldofgemconference.com](http://www.worldofgemconference.com).

**GemFest Asia Hong Kong 2008.** The GIA Alumni Association will host GemFest Asia on September 19, during the Hong Kong Jewellery & Watch Fair at the Hong Kong Convention and Exhibition Centre, Room 601. This

free educational event will feature a keynote presentation by Dr. James Shigley titled "Adventures on the Gem Trail: How GIA Research Uncovers Country of Origin." Continental breakfast will be served from 8:30 to 9:00 a.m., followed by GemFest from 9:00 to 10:30 a.m.

**Gem-A Centenary Conference and 2008 European Gemmological Symposium.** The Gemmological Association of Great Britain (Gem-A) will hold its annual conference October 25–26 in London. In conjunction with its centennial celebration, Gem-A will also be hosting this year's European Gemmological Symposium. Day one will highlight the history of gemology and the jewelry trade, and day two will discuss practical tips and new technologies for the modern gemologist. Visit [www.gem-a.info/membership/conferences.htm](http://www.gem-a.info/membership/conferences.htm).

**Gems in objects of cultural heritage.** An international conference titled *Geoarchaeology and Archaeomineralogy: Impact of Earth Sciences in the Study of Material Culture* will take place in Sofia, Bulgaria, October 29–30, 2008. One of the conference topics will be "Archaeomineralogy and Gemmology." A field trip will focus on the "Role of Bulgaria in the History of World's Jewellery Art." Visit <http://mgu.bg/docs/CircularEN.doc>.

**GIT 2008.** The Gem and Jewelry Institute of Thailand will host the *2nd International Gem & Jewelry Conference*

December 11–14 in Bangkok. The program will feature a two-day technical session, with oral and poster presentations, followed by a two-day excursion to the Kanchanaburi sapphire deposits. Abstracts are welcomed. Visit [www.git.or.th/eng/eng\\_index.htm](http://www.git.or.th/eng/eng_index.htm).

**IDCC-2.** The 2nd International Diamond Cut Conference will take place in Lausanne, Switzerland, March 22–25, 2009, just before the Basel World 2009 Jewelry and Watch Fair. A diamond cut exhibition will take place at the fair. Visit <http://idcc2.octonus.com>.

### Exhibits

**Exhibits at the GIA Museum.** From now through December 2008, "Facets of GIA" explains the various gemological services that GIA provides, including diamond grading, gem identification, education, and public outreach. The exhibit is illustrated with superb gems, crystals, and jewelry. Also currently on display in the Rosy Blue Student Commons are photo essays by Robert Weldon, manager of photography and visual communications at the GIA Library, and *Gems & Gemology* editor Brendan Laurs, depicting emerald mines in Colombia and the Paraiba-type tourmaline deposit in Mozambique, respectively (for more on the latter, see the article in the Spring 2008 issue of *G&G*). Advance reservations are required; to schedule a tour, call 760-603-4116 or e-mail [museum@gia.edu](mailto:museum@gia.edu).

## IN MEMORIAM

### GEORGE S. SWITZER (1915–2008)

Distinguished mineralogist George S. Switzer died March 23 at the age of 92.

Dr. Switzer was born in Petaluma, California, and graduated in 1937 from the University of California at Berkeley. He received a master's degree in mineralogy in 1939 and a doctorate in 1942, both from Harvard University.

After teaching at Stanford University and Harvard, Dr. Switzer served as GIA's director of research from 1946 to 1947. He published a dozen articles and news items for *Gems & Gemology* during this time and wrote several others after he left to work at the U.S. Geological Survey.

Dr. Switzer joined the Smithsonian Institution's National Museum of Natural History in 1948, where he was associate curator in the Mineralogy and Petrology Division until 1964 and chairman of the Mineral Sciences Department from 1964 to 1969. He was curator emeri-



tus until his retirement in 1975. In 1979, he and Dr. Cornelius S. Hurlbut published the classic book *Gemology*.

During his tenure at the Smithsonian, Dr. Switzer was instrumental in building the museum's National Gem Collection. In 1958, he persuaded Harry Winston to donate the legendary Hope diamond. Another highlight of his career at the Smithsonian was the purchase of one of the first electron microprobes to analyze lunar rock samples brought back from Apollo missions during the early 1970s.

In retirement, Dr. Switzer pursued his hobby of azalea propagation, eventually serving as director of the Azalea Society of America and assistant editor of its quarterly journal.

Dr. Switzer is survived by his wife of 68 years, the former Sue Bowden; two sons, Mark and James; eight grandchildren; and 12 great-grandchildren.